Circular polarization of the cosmic microwave background from vector and tensor perturbations

Keisuke Inomata[1,2] and Marc Kamionkowski[3]

[1]*ICRR, University of Tokyo, Kashiwa 277-8582, Japan*
[2]*Kavli IPMU (WPI), UTIAS, University of Tokyo, Kashiwa 277-8583, Japan*
[3]*Department of Physics and Astronomy, Johns Hopkins University, 3400 N. Charles Street, Baltimore, Maryland 21218, USA*

(Received 26 November 2018; published 4 February 2019)

Circular polarization of the cosmic microwave background (CMB) can be induced by Faraday conversion of the primordial linearly polarized radiation as it propagates through a birefringent medium. Recent work has shown that the dominant source of birefringence from primordial density perturbations is the anisotropic background CMB. Here, we extend prior work to allow for the additional birefringence that may arise from primordial vector and tensor perturbations. We derive the formulas for the power spectrum of the induced circular polarization and apply those to the standard cosmology. We find the root-variance of the induced circular polarization to be $\sqrt{\langle V^2 \rangle} \sim 3 \times 10^{-14}$ for scalar perturbations and $\sqrt{\langle V^2 \rangle} \sim 7 \times 10^{-18}(r/0.06)$ for tensor perturbations with a tensor-to-scalar ratio r.

DOI: 10.1103/PhysRevD.99.043501

I. INTRODUCTION

The cosmic microwave background (CMB) has helped us understand the history of the Universe. Through measurement of the temperature and polarization fluctuations in the CMB, we have determined precisely the classical cosmological parameters [1]. However, the temperature measurements are already limited by cosmic variance, thus motivating the investigation of other observables, such as polarization [2–4] and frequency distortions [5] of the CMB.

In this paper, we focus on the circular polarization. In astrophysics, circular polarization may arise in masers [6,7], gamma-ray-burst afterglows [8–11], jets of active galactic nuclei [12–15], and pulsars [16–19]. In addition, circular polarization has recently been discussed also in the context of the CMB [20–25]. Circular polarization can be produced through Faraday conversion when a linearly polarized light ray propagates through a medium where the indexes of refraction differ along the two different transverse axes. In this way, the linear polarization induced at the CMB last-scattering surface can be converted to circular polarization. References [20,21] discuss CMB circular polarization produced by birefringence from magnetic fields and from new physics beyond the standard model (BSM). The circular polarization produced via Faraday conversion due to supernova remnants of Population III stars is discussed in Refs. [22,23]. The current constraint to the CMB circular-polarization angular power spectrum is $l(l+1)C_l^{VV}/(2\pi) \lesssim 10^{-8}$ at multipole moments $l > 3000$ [26], $\lesssim 3 \times 10^{-11}$ at $33 < l < 307$ [27], and $\lesssim 10^{-7}$ at larger scale [28]. Forthcoming experiments, such as CLASS [29] and PIPER [30], are expected to improve considerably on the sensitivity to CMB polarization.

Recently, a detailed investigation of the circular polarization that arises from primordial perturbations was presented in Ref. [24]. No circular polarization arises at linear order, but there are several physical mechanisms that, at second order in the primordial-perturbation amplitude, can induce circular polarization from the primordial linear polarization. Although this primordially induced circular polarization may be smaller than that induced by other late-time astrophysical effects, and/or BSM physics, these predictions are more robust and may be thought of as a lower bound to the expected circular polarization. There are a number of possible standard-model sources of the cosmic birefringence needed for Faraday conversion, including, e.g., spin-polarization of hydrogen atoms induced by an anisotropic CMB background [24]. Still, the most significant source is photon-photon interactions [24,31–35], which is the mechanism we consider here. In this case, the required birefringence is provided by the CMB anisotropies seen by the CMB photon as it propagates from the surface of last scatter.

In this paper, we extend prior work by considering the additional cosmic birefringence that may be induced by primordial vector and tensor perturbations. In particular, tensor perturbations, or primordial gravitational waves, are a highly sought relic in the canonical single-field slow-roll inflationary paradigm [3,4]. Since the tensor contribution to the CMB quadrupole may be almost 10% of the total, it is conceivable—given order-unity factors—that the tensor contribution to the circular polarization may rival the scalar contribution. Note that although the photon-graviton scattering can also induce the circular polarization from tensor perturbations [36], the induced circular polarization in CMB is much smaller than that induced through photon-photon scattering as we will see later. The calculation is also valuable as an illustrative application of the total-angular-momentum (TAM) formalism [37,38] employed earlier [25] for the simpler scalar-perturbation case. In the TAM formalism, primordial perturbations are expanded in terms of TAM waves, which are eigenstates of the generators of rotations, rather than the usual plane waves (eigenstates of the generators of spatial translations). The TAM formalism allows for predictions for observables on a spherical sky to be obtained far more simply than through traditional approaches, particularly for vector and tensor perturbations.

This paper is organized as follows. In Sec. II, we introduce the basic formulas describing circular polarizations induced through the Faraday conversion. Then, we briefly review the TAM formalism in Sec. III. In Sec. IV, we take the photon-photon scattering source term as a concrete example and show how to express the source term with the TAM formalism. In Sec. V, we relate the source term to the angular power spectrum and perform numerical calculations assuming the standard cosmology. We make some concluding remarks in Sec. VI. Note that, throughout this paper, we take the Cartesian coordinate and the metric g_{ij} equals to δ_{ij}.

II. BASIC FORMULAS FOR CIRCULAR POLARIZATION

In this section, we introduce the formulas for the circular polarizations induced by Faraday conversion. Faraday conversion occurs when a light ray passes through a medium in which each axis perpendicular to the light-ray trajectory has a different index of refraction. The three-dimensional index-of-refraction tensor is given by [24]

$$n_{ij} = \delta_{ij} + \frac{1}{2}(\chi_{e,ij} + \chi_{m,ij}), \tag{1}$$

where $\chi_{e,ij}$ and $\chi_{m,ij}$ are the electric and magnetic susceptibilities, respectively. We focus on the x and y components of the tensor (z axis: photon trajectory) because photon does not have the longitudinal polarization. Then, the index-of-refraction tensor in the two-dimensional plane perpendicular to the trajectory can be expressed with four parameters as

$$n_{ab} = \begin{pmatrix} n_I + n_Q & n_U + i n_V \\ n_U - i n_V & n_I - n_Q \end{pmatrix}. \tag{2}$$

Here, n_I is the polarization-averaged index of refraction, n_Q the difference between the indexes of refraction in x and y axes in the transverse plane, and n_U is the difference between the indexes of refraction on two axes that are rotated by 45° from the x and y axes. Also, n_V is the difference between the indexes of refraction for the two different circular polarizations, which we ignore in the following because it does not convert linear polarization to circular polarization [24]. The relation between Eqs. (1) and (2) are given as $n_I = \frac{1}{2}(n_{xx} + n_{yy})$, $n_Q = \frac{1}{2}(n_{xx} - n_{yy})$, and $n_U = \frac{1}{2}(n_{xy} + n_{yx})$. In the following, we use the subscripts i, j and k to describe the three-dimensional space and use the subscripts a, b and c to describe the two-dimensional plane perpendicular to the trajectory.

An observed CMB photon has a radial trajectory that arrives from some observed direction $\hat{\boldsymbol{n}}$. According to Refs. [24,25], the circular polarization $V(\hat{\boldsymbol{n}})$ observed in direction with Stokes parameters $Q(\hat{\boldsymbol{n}})$ and $U(\hat{\boldsymbol{n}})$ at the surface of last scatter is given as

$$V(\hat{\boldsymbol{n}}) = \phi_Q(\hat{\boldsymbol{n}})U(\hat{\boldsymbol{n}}) - \phi_U(\hat{\boldsymbol{n}})Q(\hat{\boldsymbol{n}}), \tag{3}$$

where the phases $\phi_{Q,U}(\hat{\boldsymbol{n}})$ are obtained as integrals,

$$\phi_{Q,U}(\hat{\boldsymbol{n}}) = \frac{2}{c}\int_0^{\chi_{\rm LSS}} \frac{d\chi}{1+z}\omega(\chi) n_{Q,U}(\hat{\boldsymbol{n}}\chi, \eta_0 - \chi), \tag{4}$$

over comoving distance χ. Here, z is redshift, $\chi_{\rm LSS}$ is the comoving distance to the last-scattering surface and η_0 is the current conformal time. Note that a general refractive tensor is spacetime dependent as $n_{ab}(\boldsymbol{x}, \eta)$. Although the linear-polarization pattern on large angular scales is altered by reionization, the dominant contributions to the phase shift occur soon after the last scattering (see Sec. IV). Thus, the circular polarization induced after the reionization is negligible and neglected in the following.

The Stokes parameters $Q(\hat{\boldsymbol{n}})$ and $U(\hat{\boldsymbol{n}})$, as well as the phases $\phi_Q(\hat{\boldsymbol{n}})$ and $\phi_U(\hat{\boldsymbol{n}})$, are not rotational invariants; they are components (in the x-y coordinate system), respectively, of polarization and phase-shift tensors, which are, respectively, [25]

$$P_{ab}(\hat{\boldsymbol{n}}) = \frac{1}{\sqrt{2}}\begin{pmatrix} Q(\hat{\boldsymbol{n}}) & U(\hat{\boldsymbol{n}}) \\ U(\hat{\boldsymbol{n}}) & -Q(\hat{\boldsymbol{n}}) \end{pmatrix},$$
$$\Phi_{ab}(\hat{\boldsymbol{n}}) = \frac{1}{\sqrt{2}}\begin{pmatrix} \phi_Q(\hat{\boldsymbol{n}}) & \phi_U(\hat{\boldsymbol{n}}) \\ \phi_U(\hat{\boldsymbol{n}}) & -\phi_Q(\hat{\boldsymbol{n}}) \end{pmatrix}. \tag{5}$$

Then, we can rewrite Eq. (3) as

$$V(\hat{\boldsymbol{n}}) = \epsilon_{ac} P^{ab}(\hat{\boldsymbol{n}}) \Phi_b^c(\hat{\boldsymbol{n}}), \tag{6}$$

where ϵ_{ab} is the antisymmetric tensor on the 2-sphere.

III. TAM FORMALISM

In this section, we briefly review aspects of the total-angular-momentum (TAM) formalism [37,38] relevant for this work. In particular, we focus on the TAM formalism for tensor fields because the relevant anisotropies in the index of refraction are described by an index-of-refraction tensor field. Throughout this paper, we follow the notation and conventions for the TAM formalism used in Ref. [37]. In the following, we consider a symmetric trace-free tensor because, as we will see in the next section, the Faraday conversion is only related to the trace-free part of the index-of-refraction tensor.

In the usual approach, a symmetric trace-free tensor field can be expanded in terms of plane waves of helicities $\lambda = -2, \ldots, 2$ as

$$h_{ij}(\boldsymbol{x}) = \sum_{\lambda=-2}^{2} \int \frac{\mathrm{d}^3 k}{(2\pi)^3} h^\lambda(\boldsymbol{k}) (\hat{\varepsilon}^\lambda_{ij}(\hat{\boldsymbol{k}}))^* \mathrm{e}^{i\boldsymbol{k}\cdot\boldsymbol{x}}, \tag{7}$$

where the power spectra are given by

$$\langle h^\lambda(\boldsymbol{k})[h^{\lambda'}(\boldsymbol{k}')]^* \rangle = \begin{cases} \delta^{\lambda\lambda'}(2\pi)^3 \delta(\boldsymbol{k}-\boldsymbol{k}') P_L(k) & (|\lambda| = 0), \\ \delta^{\lambda\lambda'}(2\pi)^3 \delta(\boldsymbol{k}-\boldsymbol{k}') P_V(k) & (|\lambda| = 1), \\ \delta^{\lambda\lambda'}(2\pi)^3 \delta(\boldsymbol{k}-\boldsymbol{k}') P_T(k) & (|\lambda| = 2). \end{cases} \tag{8}$$

Here, $P_L(k)$, $P_V(k)$, and $P_T(k)$ are the power spectra for the longitudinal, transverse-vector, and transverse-traceless components of the tensor field, and $\hat{\varepsilon}^\lambda_{ij}$ are polarization tensors defined as [37]

$$\hat{\varepsilon}^{\pm 1}_i(\hat{\boldsymbol{k}}) = \mp \frac{1}{\sqrt{2}}(\hat{\theta}_i \mp i\hat{\phi}_i), \quad \hat{\varepsilon}^{\pm 1}_{ij}(\hat{\boldsymbol{k}}) = \frac{1}{\sqrt{2}}[\hat{\varepsilon}^{\pm 1}_i \hat{k}_j + \hat{\varepsilon}^{\pm 1}_j \hat{k}_i],$$

$$\hat{\varepsilon}^{\pm 2}_{ij}(\hat{\boldsymbol{k}}) = -\hat{\varepsilon}^{\pm 1}_i \hat{\varepsilon}^{\pm 1}_j, \qquad \hat{\varepsilon}^0_{ij}(\hat{\boldsymbol{k}}) = \sqrt{\frac{3}{2}}\left(\frac{1}{3}\delta_{ij} - \hat{k}_i \hat{k}_j\right), \tag{9}$$

where $\hat{\boldsymbol{\theta}}$ and $\hat{\boldsymbol{\phi}}$ are the transverse directions of $\hat{\boldsymbol{k}}$.

However, we can alternatively expand a symmetric trace-free tensor field in terms of total-angular-momentum (TAM) waves as [37]

$$\begin{aligned} h_{ij}(\boldsymbol{x}) &= \sum_{\lambda=0,\pm1,\pm2} \sum_{lm} \int \frac{k^2 \mathrm{d}k}{(2\pi)^3} h^{k,\lambda}_{(lm)} 4\pi i^l \Psi^{k,\lambda}_{(lm)ij}(\boldsymbol{x}) \\ &= \sum_{\alpha=L,VE,VB,TE,TB} \sum_{lm} \int \frac{k^2 \mathrm{d}k}{(2\pi)^3} h^{k,\alpha}_{(lm)} 4\pi i^l \Psi^{k,\alpha}_{(lm)ij}(\boldsymbol{x}). \end{aligned} \tag{10}$$

Here, we have written the tensor field in terms of longitudinal (L), vector-E (VE) and vector-B (VB), and tensor-E (TE) and tensor-B (TB) modes, and then also in terms of an alternative helicity basis, with $\lambda = -2, \ldots, 2$. The TAM waves are defined as

$$\Psi^{k,L}_{(lm)ij}(\boldsymbol{x}) = \sqrt{\frac{3}{2}} T^L_{ij} \Psi^k_{(lm)}(\boldsymbol{x}), \qquad \Psi^{k,VE}_{(lm)ij}(\boldsymbol{x}) = -\sqrt{\frac{2}{l(l+1)}} T^{VE}_{ij} \Psi^k_{(lm)}(\boldsymbol{x}), \qquad \Psi^{k,VB}_{(lm)ij}(\boldsymbol{x}) = -\sqrt{\frac{2}{l(l+1)}} T^{VB}_{ij} \Psi^k_{(lm)}(\boldsymbol{x}),$$

$$\Psi^{k,TE}_{(lm)ij}(\boldsymbol{x}) = -\sqrt{\frac{(l-2)!}{2(l+2)!}} T^{TE}_{ij} \Psi^k_{(lm)}(\boldsymbol{x}), \qquad \Psi^{k,TB}_{(lm)ij}(\boldsymbol{x}) = -\sqrt{\frac{(l-2)!}{2(l+2)!}} T^{TB}_{ij} \Psi^k_{(lm)}(\boldsymbol{x}), \tag{11}$$

where T^α_{ij} is defined as

$$D_i \equiv \frac{i}{k}\nabla_i, \qquad L_i \equiv -ir\epsilon_{ijk}\hat{n}^j \nabla^k, \qquad K_i \equiv -iL_i, \qquad M_{\perp,i} \equiv \epsilon_{ijk} D^j K^k, \qquad T^L_{ij} \equiv -D_i D_j + \frac{1}{3}\delta_{ij}, \qquad T^{VE}_{ij} \equiv D_{(i} M_{j)},$$

$$T^{VB}_{ij} \equiv D_{(i} K_{j)}, \qquad T^{TE}_{ij} \equiv M_{(i} M_{j)} - K_{(i} K_{j)} + 2D_{(i} M_{j)}, \qquad T^{TB}_{ij} \equiv K_{(i} M_{j)} + M_{(i} K_{j)} + 2D_{(i} K_{j)}, \tag{12}$$

and $\Psi^k_{(lm)}(\boldsymbol{x}) = j_l(k\chi) Y_{(lm)}(\hat{\boldsymbol{n}})(\boldsymbol{x} = \chi\hat{\boldsymbol{n}})$ are scalar TAM waves, written in terms of the spherical Bessel function $j_l(x)$ and spherical harmonic $Y_{(lm)}(\hat{\boldsymbol{n}})$.

The helicity-basis TAM waves are then

$$\Psi^{k,0}_{(lm)ij}(\boldsymbol{x}) = \Psi^{k,L}_{(lm)ij}(\boldsymbol{x}), \qquad \Psi^{k,\pm1}_{(lm)ij}(\boldsymbol{x}) = \frac{1}{\sqrt{2}}[\Psi^{k,VE}_{(lm)ij}(\boldsymbol{x}) \pm i\Psi^{k,VB}_{(lm)ij}(\boldsymbol{x})], \qquad \Psi^{k,\pm2}_{(lm)ij}(\boldsymbol{x}) = \frac{1}{\sqrt{2}}[\Psi^{k,TE}_{(lm)ij}(\boldsymbol{x}) \pm i\Psi^{k,TB}_{(lm)ij}(\boldsymbol{x})]. \tag{13}$$

The relations between $h^{k,\lambda}_{(lm)}$ and $h^{k,\alpha}_{(lm)}$ are given by

$$h^{k,0}_{(lm)} = h^{k,L}_{(lm)}, \qquad h^{k,\pm1}_{(lm)} = \frac{1}{\sqrt{2}}[h^{k,VE}_{(lm)} \mp ih^{k,VB}_{(lm)}], \qquad h^{k,\pm2}_{(lm)} = \frac{1}{\sqrt{2}}[h^{k,TE}_{(lm)} \mp ih^{k,TB}_{(lm)}]. \tag{14}$$

The plane waves with an arbitrary trace-free polarization tensor $\hat{\varepsilon}_{ij}$, which is a combination of $\hat{\varepsilon}^{\lambda}_{ij}$ or $\hat{\varepsilon}^{\alpha}_{ij}$ in general and can be $\hat{\varepsilon}^{\lambda}_{ij}$ or $\hat{\varepsilon}^{\alpha}_{ij}$ themselves in some cases, are related to the TAM basis functions as [37]

$$\hat{\varepsilon}_{ij}(\hat{\boldsymbol{k}})\mathrm{e}^{i\boldsymbol{k}\cdot\boldsymbol{x}} = \sum_{\alpha}\sum_{lm} 4\pi i^l B^{\alpha}_{(lm)}(\hat{\boldsymbol{k}})\Psi^{k,\alpha}_{(lm)ij}(\boldsymbol{x}) = \sum_{\lambda=0,\pm1,\pm2}\sum_{lm} 4\pi i^l B^{\lambda}_{(lm)}(\hat{\boldsymbol{k}})\Psi^{k,\lambda}_{(lm)ij}(\boldsymbol{x}), \tag{15}$$

where α runs over L, VE, VB, TE, TB, and

$$B^{\alpha}_{(lm)}(\hat{\boldsymbol{k}}) = \hat{\varepsilon}^{ij}(\hat{\boldsymbol{k}})Y^{\alpha*}_{(lm)ij}(\hat{\boldsymbol{k}}), \qquad B^{\lambda}_{(lm)}(\hat{\boldsymbol{k}}) = \hat{\varepsilon}^{ij}(\hat{\boldsymbol{k}})Y^{\lambda*}_{(lm)ij}(\hat{\boldsymbol{k}}). \tag{16}$$

The tensor spherical harmonics $Y^{\alpha}_{(lm)ij}(\hat{\boldsymbol{n}})$ are defined as[1]

$$\begin{aligned}
&Y^{L}_{(lm)ij}(\hat{\boldsymbol{n}}) = \sqrt{\frac{3}{2}}W^{L}_{ij}Y_{(lm)}(\hat{\boldsymbol{n}}),\\
&Y^{VE}_{(lm)ij}(\hat{\boldsymbol{n}}) = -\sqrt{\frac{2}{l(l+1)}}W^{VE}_{ij}Y_{(lm)}(\hat{\boldsymbol{n}}), \qquad Y^{VB}_{(lm)ij}(\hat{\boldsymbol{n}}) = -\sqrt{\frac{2}{l(l+1)}}W^{VB}_{ij}Y_{(lm)}(\hat{\boldsymbol{n}}),\\
&Y^{TE}_{(lm)ij}(\hat{\boldsymbol{n}}) = -\sqrt{\frac{(l-2)!}{2(l+2)!}}W^{TE}_{ij}Y_{(lm)}(\hat{\boldsymbol{n}}), \qquad Y^{TB}_{(lm)ij}(\hat{\boldsymbol{n}}) = -\sqrt{\frac{(l-2)!}{2(l+2)!}}W^{TB}_{ij}Y_{(lm)}(\hat{\boldsymbol{n}}),
\end{aligned} \tag{17}$$

where W^{α}_{ij} is defined as

$$\begin{aligned}
&N_i \equiv -\hat{n}_i, \qquad K_i \equiv -iL_i, \qquad M_{\perp i} \equiv \epsilon_{ijk}N^jK^k \qquad W^{L}_{ij} \equiv -N_iN_j + \frac{1}{3}\delta_{ij}, \qquad W^{VE}_{ij} \equiv N_{(i}M_{\perp j)}, \qquad W^{VB}_{ij} \equiv N_{(i}K_{j)},\\
&W^{TE}_{ij} \equiv M_{\perp(i}M_{\perp j)} - K_{(i}K_{j)} + 2N_{(i}M_{\perp j)}, \qquad W^{TB}_{ij} \equiv K_{(i}M_{\perp j)} + M_{\perp(i}K_{j)} + 2N_{(i}K_{j)}.
\end{aligned} \tag{18}$$

In particular, $Y^{TE}_{(lm)ij}$ and $Y^{TB}_{(lm)ij}$ live in the plane perpendicular to $\hat{\boldsymbol{n}}$ and can be expressed as $Y^{TE}_{(lm)ab}$ and $Y^{TB}_{(lm)ab}$, respectively. The helicity-basis spherical harmonics $Y^{\lambda}_{(lm)ij}(\hat{\boldsymbol{n}})$ are defined as

$$Y^{0}_{(lm)ij}(\hat{\boldsymbol{n}}) = Y^{L}_{(lm)ij}(\hat{\boldsymbol{n}}), \qquad Y^{\pm1}_{(lm)ij}(\hat{\boldsymbol{n}}) = \frac{1}{\sqrt{2}}[Y^{VE}_{(lm)ij}(\hat{\boldsymbol{n}}) \pm iY^{VB}_{(lm)ij}(\hat{\boldsymbol{n}})], \qquad Y^{\pm2}_{(lm)ij}(\hat{\boldsymbol{n}}) = \frac{1}{\sqrt{2}}[Y^{TE}_{(lm)ij}(\hat{\boldsymbol{n}}) \pm iY^{TB}_{(lm)ij}(\hat{\boldsymbol{n}})]. \tag{19}$$

The $Y^{\lambda}_{(lm)ij}(\hat{\boldsymbol{k}})$ are related to the spin-weighted spherical harmonics by [39,40]

$$\hat{\varepsilon}^{ij}_{\lambda}(\hat{\boldsymbol{k}})Y^{\lambda'}_{(lm)ij}(\hat{\boldsymbol{k}}) = {}_{-\lambda}Y_{(lm)}(\hat{\boldsymbol{k}})\delta^{\lambda'}_{\lambda}. \tag{20}$$

From Eqs. (7), (10), and (20), we can derive the following relations between $h^{\lambda}(\boldsymbol{k})$ and $h^{k,\lambda}_{(lm)}$:

$$h^{k,\lambda}_{(lm)} = \int \mathrm{d}\hat{\boldsymbol{k}}\, h^{\lambda}(\boldsymbol{k})({}_{-\lambda}Y_{(lm)}(\hat{\boldsymbol{k}}))^*. \tag{21}$$

As a result, the TAM amplitudes satisfy[2]

$$\langle h^{k,\lambda}_{(lm)}[h^{k',\lambda'}_{(l'm')}]^*\rangle = \begin{cases} \delta_{ll'}\delta_{mm'}\delta^{\lambda\lambda'}\frac{(2\pi)^3}{k^2}\delta(k-k')P_L(k) & (|\lambda|=0),\\ \delta_{ll'}\delta_{mm'}\delta^{\lambda\lambda'}\frac{(2\pi)^3}{k^2}\delta(k-k')P_V(k) & (|\lambda|=1),\\ \delta_{ll'}\delta_{mm'}\delta^{\lambda\lambda'}\frac{(2\pi)^3}{k^2}\delta(k-k')P_T(k) & (|\lambda|=2),\end{cases} \tag{22}$$

[1]The two components that live in the plane of the sky, which we here refer to as TE and TB modes, are in much of the literature (which considers only these two components) as E and B.

[2]The spin-weighted spherical harmonics satisfy $\int \mathrm{d}\hat{\boldsymbol{n}}\,{}_{\lambda}Y_{(lm)}(\hat{\boldsymbol{n}})\,{}_{\lambda'}Y^*_{(l'm')}(\hat{\boldsymbol{n}}) = \delta_{ll'}\delta_{mm'}\delta_{\lambda\lambda'}$.

$$\langle h^{k,\alpha}_{(lm)}[h^{k',\alpha'}_{(l'm')}]^*\rangle = \begin{cases} \delta_{ll'}\delta_{mm'}\delta^{\alpha\alpha'}\frac{(2\pi)^3}{k^2}\delta(k-k')P_L(k) & (\alpha = L), \\ \delta_{ll'}\delta_{mm'}\delta^{\alpha\alpha'}\frac{(2\pi)^3}{k^2}\delta(k-k')P_V(k) & (\alpha = VE, VB), \\ \delta_{ll'}\delta_{mm'}\delta^{\alpha\alpha'}\frac{(2\pi)^3}{k^2}\delta(k-k')P_T(k) & (\alpha = TE, TB). \end{cases} \tag{23}$$

IV. CALCULATION OF $\Phi_{ab}(\hat{n})$

Although there are several physical effects that may generate Faraday conversion, the dominant mechanism, as noted in Ref. [24], is photon-photon scattering. The components of the index-of-refraction tensor due to photon-photon scattering is (see Appendix B and Ref. [24] for the derivation),

$$n_Q(\boldsymbol{x},\eta) \equiv \frac{1}{2}(n_{xx}(\boldsymbol{x},\eta) - n_{yy}(\boldsymbol{x},\eta)) \simeq 48\sqrt{\frac{\pi}{5}}A_e\mu_0 a_{\rm rad}T^4_{\rm CMB}{\rm Re}a^E_{2,-2}(\boldsymbol{x},\eta), \tag{24}$$

$$n_U(\boldsymbol{x},\eta) \equiv \frac{1}{2}(n_{xy}(\boldsymbol{x},\eta) + n_{yx}(\boldsymbol{x},\eta)) \simeq 48\sqrt{\frac{\pi}{5}}A_e\mu_0 a_{\rm rad}T^4_{\rm CMB}{\rm Im}a^E_{2,-2}(\boldsymbol{x},\eta). \tag{25}$$

Here, μ_0 is the magnetic permeability of the vacuum, $a_{\rm rad}$ is the radiation energy density constant, $T_{\rm CMB}$ is the CMB temperature, $a^E_{lm}(\boldsymbol{x},\eta)$ is the coefficient of the local E-mode moment induced by primordial perturbations, and A_e is the Euler-Heisenberg interaction constant, which can be expressed with electron mass m_e, Compton wavelength λ_e, and the fine structure constant α as $A_e = 2\alpha^2\lambda_e^3/(45\mu_0 m_e c^2)$. Next, we write the spatial dependence of the indexes of refraction in terms of Fourier components through

$$n_Q(\boldsymbol{x},\eta) \simeq 48\sqrt{\frac{\pi}{5}}A_e\mu_0 a_{\rm rad}T^4_{\rm CMB}\frac{1}{2}\int\frac{{\rm d}^3k}{(2\pi)^3}(a^E_{2,-2}(\boldsymbol{k},\eta) + a^E_{2,2}(\boldsymbol{k},\eta)){\rm e}^{i\boldsymbol{k}\cdot\boldsymbol{x}}, \tag{26}$$

$$n_U(\boldsymbol{x},\eta) \simeq 48\sqrt{\frac{\pi}{5}}A_e\mu_0 a_{\rm rad}T^4_{\rm CMB}\frac{1}{2i}\int\frac{{\rm d}^3k}{(2\pi)^3}(a^E_{2,-2}(\boldsymbol{k},\eta) - a^E_{2,2}(\boldsymbol{k},\eta)){\rm e}^{i\boldsymbol{k}\cdot\boldsymbol{x}}, \tag{27}$$

where we have used the relation $a^{E*}_{22} = a^E_{2,-2}$. We then transform the local quadrupole moments in Eqs. (26) and (27) using

$$a^E_{2,\pm2}(\boldsymbol{k},\eta) = \sum_{m=0,\pm1,\pm2} D^2_{\pm2,m}(\pi-\phi_{\boldsymbol{k}},\theta_{\boldsymbol{k}},0)\bar{a}^E_{2,m}(\boldsymbol{k},\eta), \tag{28}$$

where unbarred quantities are in the line-of-sight frame (with the z axis toward the observer), and barred quantities are in the wave vector frame ($\boldsymbol{k}$ is the z axis and the direction toward the observer in the $\bar{x}\,\bar{z}$ plane, with $\bar{x} < 0$). Here, $\theta_{\boldsymbol{k}}$ and $\phi_{\boldsymbol{k}}$ are the polar and azimuthal angle of $\hat{\boldsymbol{k}}$ in the line-of-sight frame, and $D^l_{m'm}$ is the Wigner rotation matrix, which is defined in Eq. (A1). Then, we derive

$$\begin{aligned} a^E_{2,-2}(\boldsymbol{k},\eta) + a^E_{22}(\boldsymbol{k},\eta) &= \sum_m D^2_{-2,m}(\pi-\phi_{\boldsymbol{k}},\theta_{\boldsymbol{k}},0)\bar{a}^E_{2,m}(\boldsymbol{k},\eta) + \sum_m D^2_{2,m}(\pi-\phi_{\boldsymbol{k}},\theta_{\boldsymbol{k}},0)\bar{a}^E_{2,m}(\boldsymbol{k},\eta) \\ &= \sqrt{\frac{3}{2}}(\cos\phi^2_{\boldsymbol{k}} - \sin\phi^2_{\boldsymbol{k}})\sin\theta^2_{\boldsymbol{k}}\bar{a}^E_{2,0}(\boldsymbol{k},\eta) - \sin\theta_{\boldsymbol{k}}(-\cos\theta_{\boldsymbol{k}}\cos 2\phi_{\boldsymbol{k}} + i\sin 2\phi_{\boldsymbol{k}})\bar{a}^E_{2,1}(\boldsymbol{k},\eta) \\ &\quad - \sin\theta_{\boldsymbol{k}}(\cos\theta_{\boldsymbol{k}}\cos 2\phi_{\boldsymbol{k}} + i\sin 2\phi_{\boldsymbol{k}})\bar{a}^E_{2,-1}(\boldsymbol{k},\eta) \\ &\quad + \left(\frac{3+\cos 2\theta_{\boldsymbol{k}}}{4}\cos 2\phi_{\boldsymbol{k}} - i\cos\theta_{\boldsymbol{k}}\sin 2\phi_{\boldsymbol{k}}\right)\bar{a}^E_{2,2}(\boldsymbol{k},\eta) \\ &\quad + \left(\frac{3+\cos 2\theta_{\boldsymbol{k}}}{4}\cos 2\phi_{\boldsymbol{k}} + i\cos\theta_{\boldsymbol{k}}\sin 2\phi_{\boldsymbol{k}}\right)\bar{a}^E_{2,-2}(\boldsymbol{k},\eta) \\ &= -((\hat{\varepsilon}^0_{xx}(\hat{\boldsymbol{k}}))^* - (\hat{\varepsilon}^0_{yy}(\hat{\boldsymbol{k}}))^*)\bar{a}^E_{2,0}(\boldsymbol{k},\eta) - ((\hat{\varepsilon}^{+1}_{xx}(\hat{\boldsymbol{k}}))^* - (\hat{\varepsilon}^{+1}_{yy}(\hat{\boldsymbol{k}}))^*)\bar{a}^E_{2,1}(\boldsymbol{k},\eta) \\ &\quad - ((\hat{\varepsilon}^{-1}_{xx}(\hat{\boldsymbol{k}}))^* - (\hat{\varepsilon}^{-1}_{yy}(\hat{\boldsymbol{k}}))^*)\bar{a}^E_{2,-1}(\boldsymbol{k},\eta) - ((\hat{\varepsilon}^{+2}_{xx}(\hat{\boldsymbol{k}}))^* - (\hat{\varepsilon}^{+2}_{yy}(\hat{\boldsymbol{k}}))^*)\bar{a}^E_{2,2}(\boldsymbol{k},\eta) \\ &\quad - ((\hat{\varepsilon}^{-2}_{xx}(\hat{\boldsymbol{k}}))^* - (\hat{\varepsilon}^{-2}_{yy}(\hat{\boldsymbol{k}}))^*)\bar{a}^E_{2,-2}(\boldsymbol{k},\eta), \end{aligned} \tag{29}$$

$$\begin{aligned}\frac{1}{i}(a^E_{2,-2}(\boldsymbol{k},\eta)-a^E_{2,2}(\boldsymbol{k},\eta)) &= \frac{1}{i}\left(\sum_m D^2_{-2,m}(\pi-\phi_{\boldsymbol{k}},\theta_{\boldsymbol{k}},0)\bar{a}^E_{2,m}(\boldsymbol{k},\eta)-\sum_m D^2_{2,m}(\pi-\phi_{\boldsymbol{k}},\theta_{\boldsymbol{k}},0)\bar{a}^E_{2,m}(\boldsymbol{k},\eta)\right)\\
&= \sqrt{6}\cos\phi_{\boldsymbol{k}}\sin\phi_{\boldsymbol{k}}\sin\theta^2_{\boldsymbol{k}}\bar{a}^E_{2,0}(\boldsymbol{k},\eta)+\sin\theta_{\boldsymbol{k}}(i\cos 2\phi_{\boldsymbol{k}}+\cos\theta\sin 2\phi_{\boldsymbol{k}})\bar{a}^E_{2,1}(\boldsymbol{k},\eta)\\
&\quad+\sin\theta_{\boldsymbol{k}}(i\cos 2\phi_{\boldsymbol{k}}-\cos\theta_{\boldsymbol{k}}\sin 2\phi_{\boldsymbol{k}})\bar{a}^E_{2,-1}(\boldsymbol{k},\eta)\\
&\quad+\left(\frac{3+\cos 2\theta_{\boldsymbol{k}}}{4}\sin 2\phi_{\boldsymbol{k}}+i\cos\theta_{\boldsymbol{k}}\cos 2\phi_{\boldsymbol{k}}\right)\bar{a}^E_{2,2}(\boldsymbol{k},\eta)\\
&\quad+\left(\frac{3+\cos 2\theta_{\boldsymbol{k}}}{4}\sin 2\phi_{\boldsymbol{k}}-i\cos\theta_{\boldsymbol{k}}\cos 2\phi_{\boldsymbol{k}}\right)\bar{a}^E_{2,-2}(\boldsymbol{k},\eta)\\
&= -2(\hat{\varepsilon}^0_{xy}(\hat{\boldsymbol{k}}))^*\bar{a}^E_{2,0}(\boldsymbol{k},\eta)-2(\hat{\varepsilon}^{+1}_{xy}(\hat{\boldsymbol{k}}))^*\bar{a}^E_{2,1}(\boldsymbol{k},\eta)-2(\hat{\varepsilon}^{-1}_{xy}(\hat{\boldsymbol{k}}))^*\bar{a}^E_{2,-1}(\boldsymbol{k},\eta)\\
&\quad-2(\hat{\varepsilon}^{+2}_{xy}(\hat{\boldsymbol{k}}))^*\bar{a}^E_{2,2}(\boldsymbol{k})-2(\hat{\varepsilon}^{-2}_{xy}(\hat{\boldsymbol{k}}))^*\bar{a}^E_{2,-2}(\boldsymbol{k},\eta),\end{aligned} \tag{30}$$

where $\hat{\varepsilon}^\lambda_{ij}$ is defined by Eq. (9), and the basis vectors are

$$\hat{\boldsymbol{\theta}}(\hat{\boldsymbol{k}})=(\cos\theta_{\boldsymbol{k}}\cos\phi_{\boldsymbol{k}},\cos\theta_{\boldsymbol{k}}\sin\phi_{\boldsymbol{k}},-\sin\theta_{\boldsymbol{k}}),\qquad \hat{\boldsymbol{\phi}}(\hat{\boldsymbol{k}})=(-\sin\phi_{\boldsymbol{k}},\cos\phi_{\boldsymbol{k}},0). \tag{31}$$

Here, we separate the primordial perturbations and their transfer functions through $\bar{a}^E_{2,\lambda}(\boldsymbol{k},\eta)=\bar{a}^E_{2,\lambda}(k,\eta)h^\lambda(\boldsymbol{k})$, where the power spectra of $h^\lambda(\boldsymbol{k})$ are given by Eq. (8).

From Eqs. (24), (25), (29), and (30), we see that the part of n_{ij} proportional to $(\hat{\varepsilon}^\lambda_{ij})^*$ can describe n_Q and n_U, which means that the part related to n_Q and n_U in n_{ij} can be expressed with a trace-free tensor, given as Eq. (7). On the other hand, a nonzero-trace part of n_{ij} is irrelevant to n_Q or n_U. Using the relation between $(\hat{\varepsilon}^\lambda_{ij})^*$ and $\Psi^{k,\lambda}_{(lm)ij}$ given in Eq. (15), we can express n_{ij} as

$$n_{ij}(\boldsymbol{x},\eta)=48\sqrt{\frac{\pi}{5}}A_e\mu_0 a_{\rm rad}T^4_{\rm CMB}\int\frac{k^2{\rm d}k}{(2\pi)^3}\sum_{lm}\sum_{\lambda=0,\pm1,\pm2}4\pi i^l\Psi^{k,\lambda}_{(lm)ij}(\boldsymbol{x})h^{k,\lambda}_{(lm)}(-\bar{a}^E_{2,\lambda}(k,\eta))+\tilde{n}_{ij}(\boldsymbol{x},\eta) \tag{32}$$

$$\begin{aligned}&=48\sqrt{\frac{\pi}{5}}A_e\mu_0 a_{\rm rad}T^4_{\rm CMB}\int\frac{k^2{\rm d}k}{(2\pi)^3}\sum_{lm}4\pi i^l(\Psi^{k,L}_{(lm)ij}(\boldsymbol{x})h^{k,L}_{(lm)}(-\bar{a}^E_{2,0}(k,\eta))\\
&\quad+\Psi^{k,VE}_{(lm)ij}(\boldsymbol{x})h^{k,VE}_{(lm)}(-\bar{a}^E_{2,1}(k,\eta))+\Psi^{k,VB}_{(lm)ij}(\boldsymbol{x})h^{k,VB}_{(lm)}(-\bar{a}^E_{2,1}(k,\eta))\\
&\quad+\Psi^{k,TE}_{(lm)ij}(\boldsymbol{x})h^{k,TE}_{(lm)}(-\bar{a}^E_{2,2}(k,\eta))+\Psi^{k,TB}_{(lm)ij}(\boldsymbol{x})h^{k,TB}_{(lm)}(-\bar{a}^E_{2,2}(k,\eta)))+\tilde{n}_{ij}(\boldsymbol{x},\eta),\end{aligned} \tag{33}$$

where $\tilde{n}_{ij}$ is the part of n_{ij} that is independent of n_Q or n_U, and we have used the relation $\bar{a}^E_{2,\lambda}(k,\eta)=\bar{a}^E_{2,-\lambda}(k,\eta)$ [41].

To calculate the induced circular polarization, we need to derive $\Phi_{ab}(\hat{\boldsymbol{n}})$ from $n_{ij}(\boldsymbol{x})$. Since P_{ab} and Φ_{ab} are 2×2 symmetric trace-free tensors in the celestial sphere, we can expand them in terms of $Y^{TE}_{(lm)ab}(\hat{\boldsymbol{n}})$ and $Y^{TB}_{(lm)ab}(\hat{\boldsymbol{n}})$ as [42,43],

$$P_{ab}(\hat{\boldsymbol{n}})=\sum_{lm}[P^E_{lm}Y^{TE}_{(lm)ab}(\hat{\boldsymbol{n}})+P^B_{lm}Y^{TB}_{(lm)ab}(\hat{\boldsymbol{n}})], \tag{34}$$

$$\Phi_{ab}(\hat{\boldsymbol{n}})=\sum_{lm}[\Phi^E_{lm}Y^{TE}_{(lm)ab}(\hat{\boldsymbol{n}})+\Phi^B_{lm}Y^{TB}_{(lm)ab}(\hat{\boldsymbol{n}})]. \tag{35}$$

To relate $n_{ij}(\boldsymbol{x})$ to the shift tensor $\Phi_{ab}(\hat{\boldsymbol{n}})$, we define the projection operator $\Lambda^{kl}_{ij}(\hat{\boldsymbol{n}})$ to project $n_{ij}(\boldsymbol{x})$ to a spin-2 tensor on the celestial sphere as

$$\Lambda_{ij}{}^{kl}(\hat{\boldsymbol{n}})\equiv P_i{}^kP_j{}^l-\frac{1}{2}P^{mk}P_m{}^l\delta_{ij}, \tag{36}$$

where P_{ij} is given as $P_{ij}=\delta_{ij}-\hat{n}_i\hat{n}_j$. Then, we can express the shift tensor in terms of $n_{ij}(\boldsymbol{x})$ as [25]

$$\Phi_{ij}(\hat{\boldsymbol{n}}) = \frac{\omega_0}{\sqrt{2}}\frac{2}{c}\int_0^{\chi_{\rm LSS}} \mathrm{d}\chi [\Lambda_{ij}{}^{k'l'}(\hat{\boldsymbol{n}}) n_{k'l'}(\hat{\boldsymbol{n}}\chi, \eta_0 - \chi)], \tag{37}$$

where ω_0 is the frequency today. Note that since Φ_{ij} lives on the plane perpendicular to $\hat{\boldsymbol{n}}$, we can regard Φ_{ij} as Φ_{ab}[3] and, by definition, $\Lambda_{ij}{}^{k'l'}\tilde{n}_{k'l'} = 0$ is satisfied. As we found in Eq. (33), the spatial dependence of $n_{ij}(\boldsymbol{x})$ can be expressed with $\Psi^{k,\lambda}_{(lm)ij}(\boldsymbol{x})$ and the projection of $\Psi^{k,\lambda}_{(lm)ij}(\boldsymbol{x})$ onto the celestial sphere is discussed in Refs. [25,37]. According to Eq. (94) in Ref. [37], $\Lambda_{ij}{}^{k'l'}\Psi^{\lambda}_{k'l'}(\hat{\boldsymbol{n}}\chi)$ are given by

$$\Lambda_{ij}{}^{k'l'}(\hat{\boldsymbol{n}})\Psi^{k,L}_{(lm)k'l'}(\hat{\boldsymbol{n}}\chi) = -\frac{\sqrt{3}}{2}\sqrt{\frac{(l+2)!}{(l-2)!}}\frac{j_l(k\chi)}{(k\chi)^2}Y^{TE}_{(lm)ij}(\hat{\boldsymbol{n}}) \equiv -\sqrt{2}\epsilon^{(0)}_l(k\chi)Y^{TE}_{(lm)ij}(\hat{\boldsymbol{n}}), \tag{38}$$

$$\Lambda_{ij}{}^{k'l'}(\hat{\boldsymbol{n}})\Psi^{k,VE}_{(lm)k'l'}(\hat{\boldsymbol{n}}\chi) = -\sqrt{(l-1)(l+2)}\left(f_l(k\chi) + 2\frac{j_l(k\chi)}{(k\chi)^2}\right)Y^{TE}_{(lm)ij}(\hat{\boldsymbol{n}}) \equiv -2\epsilon^{(1)}_l(k\chi)Y^{TE}_{(lm)ij}(\hat{\boldsymbol{n}}), \tag{39}$$

$$\Lambda_{ij}{}^{k'l'}(\hat{\boldsymbol{n}})\Psi^{k,TE}_{(lm)k'l'}(\hat{\boldsymbol{n}}\chi) = -\frac{1}{2}\left(-j_l(k\chi) + g_l(k\chi) + 4f_l(k\chi) + 6\frac{j_l(k\chi)}{(k\chi)^2}\right)Y^{TE}_{(lm)ij}(\hat{\boldsymbol{n}}) \equiv -2\epsilon^{(2)}_l(k\chi)Y^{TE}_{(lm)ij}(\hat{\boldsymbol{n}}), \tag{40}$$

$$\Lambda_{ij}{}^{k'l'}(\hat{\boldsymbol{n}})\Psi^{k,VB}_{(lm)k'l'}(\hat{\boldsymbol{n}}\chi) = -i\sqrt{(l-1)(l+2)}\frac{j_l(k\chi)}{k\chi}Y^{TB}_{(lm)ij}(\hat{\boldsymbol{n}}) \equiv -2i\beta^{(1)}_l(k\chi)Y^{TB}_{(lm)ij}(\hat{\boldsymbol{n}}), \tag{41}$$

$$\Lambda^{k'l'}_{ij}(\hat{\boldsymbol{n}})\Psi^{k,TB}_{(lm)k'l'}(\hat{\boldsymbol{n}}\chi) = -i\left(j'_l(k\chi) + 2\frac{j_l(k\chi)}{k\chi}\right)Y^{TB}_{(lm)ij}(\hat{\boldsymbol{n}}) \equiv -2i\beta^{(2)}_l(k\chi)Y^{TB}_{(lm)ij}(\hat{\boldsymbol{n}}), \tag{42}$$

where $f_l(x) \equiv \frac{\mathrm{d}}{\mathrm{d}x}\frac{j_l(x)}{x}$, $g_l(x) \equiv -j_l(x) - 2f_l(x) + (l-1)(l+2)\frac{j_l(x)}{x^2}$ and $\epsilon^{(m)}_l(x)$ and $\beta^{(m)}_l(x)$ are defined as in Ref. [41]. Note again that since $Y^{TE}_{(lm)ij}$ and $Y^{TB}_{(lm)ij}$ can be described in the plane perpendicular to $\hat{\boldsymbol{n}}$, we can regard them as $Y^{TE}_{(lm)ab}$ and $Y^{TB}_{(lm)ab}$, respectively.

From Eqs. (37)–(42) for $\Phi^{E/B}_{lm}$ and Ref. [44] for $P^{E/B}_{lm}$, we can rewrite the coefficients in Eqs. (34) and (35) as[4]

$$P^{E/B}_{lm} = \sum_\alpha P^{E/B,\lambda}_{lm}, \qquad \Phi^{E/B}_{lm} = \sum_\alpha \Phi^{E/B,\lambda}_{lm}, \tag{43}$$

$$P^{E,L}_{lm} = 4\pi\int\frac{k^2\mathrm{d}k}{(2\pi)^3}\int_0^{\eta_0}\mathrm{d}\eta g(\eta)(-\sqrt{6}\mathcal{P}^{(0)}(k,\eta))h^{k,(L)}_{lm}\epsilon^{(0)}_l(k(\eta_0-\eta)), \tag{44}$$

$$P^{E/B,VE/VB}_{lm} = 4\pi\int\frac{k^2\mathrm{d}k}{(2\pi)^3}\int_0^{\eta_0}\mathrm{d}\eta g(\eta)\sqrt{2}(-\sqrt{6}\mathcal{P}^{(1)}(k,\eta))h^{k,(VE/VB)}_{lm}\phi^{(1)}_l(k(\eta_0-\eta)), \tag{45}$$

$$P^{E/B,TE/TB}_{lm} = 4\pi\int\frac{k^2\mathrm{d}k}{(2\pi)^3}\int_0^{\eta_0}\mathrm{d}\eta g(\eta)\sqrt{2}(-\sqrt{6}\mathcal{P}^{(2)}(k,\eta))h^{k,(TE/TB)}_{lm}\phi^{(2)}_l(k(\eta_0-\eta)), \tag{46}$$

$$\Phi^{E,L}_{lm} = 4\pi A\int\frac{k^2\mathrm{d}k}{(2\pi)^3}\int_{\eta_{\rm LSS}}^{\eta_0}\mathrm{d}\eta(1+z)^4(\bar{a}^E_{2,0}(k,\eta))h^{k,(L)}_{lm}\epsilon^{(0)}_l(k(\eta_0-\eta)), \tag{47}$$

$$\Phi^{E/B,VE/VB}_{lm} = 4\pi A\int\frac{k^2\mathrm{d}k}{(2\pi)^3}\int_{\eta_{\rm LSS}}^{\eta_0}\mathrm{d}\eta(1+z)^4\sqrt{2}(\bar{a}^E_{2,1}(k,\eta))h^{k,(VE/VB)}_{lm}\phi^{(1)}_l(k(\eta_0-\eta)), \tag{48}$$

[3] In the line-of-sight frame, $\hat{\boldsymbol{n}}$ is parallel to z axis and a and b run over x-y plane in the three-dimensional Cartesian coordinate. In other words, Φ_{ij} is nonzero only for $i, j \neq z$ in that frame.

[4] Note that Eq. (46) corrects Eq. (30) in Ref. [25].

$$\Phi_{lm}^{E/B,TE/TB} = 4\pi A \int \frac{k^2 \mathrm{d}k}{(2\pi)^3} \int_{\eta_{\rm LSS}}^{\eta_0} \mathrm{d}\eta (1+z)^4 \sqrt{2} (\bar{a}^E_{2,2}(k,\eta)) h_{lm}^{k,(TE/TB)} \phi_l^{(2)}(k(\eta_0-\eta)), \tag{49}$$

where the integration variable is changed as $\chi \to \eta$ ($\eta = \eta_0 - \chi$), $\phi^m(x)$ is $\epsilon^m(x)$ for VE and TE or $i\beta^m(x)$ for VB and TB, $g(\eta)$ is the visibility function, $\mathcal{P}^{(m)}(k,\eta)$ is the function defined in Ref. [44], and $A \equiv 96(\pi/5)^{1/2} A_e \mu_0 a_{\rm rad} T_0^4 c^{-1} \omega_0 = 1.11 \times 10^{-38} (\nu_0/100~\mathrm{GHz})\,\mathrm{m}^{-1}$ [24]. The power spectra of $h_{lm}^{k,\alpha}$ are given by Eq. (23). The factor of $(1+z)^4$ implies that the dominant contribution to the phase shift is near the epoch of recombination, as we mentioned in Sec. II.

Finally, we summarize the results for the angular power spectra. We can express $C_l^{P^E P^E}$ and $C_l^{P^B P^B}$ as

$$\begin{aligned} C_l^{P^E P^E} = \sum_{\alpha = L,VE,TE} \langle P_{lm}^{E,(\alpha)*} P_{lm}^{E,(\alpha)} \rangle &= 4\pi \int \frac{\mathrm{d}k}{k} \left(\frac{k^3}{2\pi^2} P^{(L)}(k) \right) \left| \int_0^{\eta_0} \mathrm{d}\eta g(\eta) (-\sqrt{6} \mathcal{P}^{(0)}(k,\eta)) \epsilon_l^{(0)}(k(\eta_0-\eta)) \right|^2 \\ &+ 4\pi \int \frac{\mathrm{d}k}{k} 2 \left(\frac{k^3}{2\pi^2} P^{(VE)}(k) \right) \left| \int_0^{\eta_0} \mathrm{d}\eta g(\eta) (-\sqrt{6} \mathcal{P}^{(1)}(k,\eta)) \epsilon_l^{(1)}(k(\eta_0-\eta)) \right|^2 \\ &+ 4\pi \int \frac{\mathrm{d}k}{k} 2 \left(\frac{k^3}{2\pi^2} P^{(TE)}(k) \right) \left| \int_0^{\eta_0} \mathrm{d}\eta g(\eta) (-\sqrt{6} \mathcal{P}^{(2)}(k,\eta)) \epsilon_l^{(2)}(k(\eta_0-\eta)) \right|^2, \end{aligned} \tag{50}$$

$$\begin{aligned} C_l^{P^B P^B} = \sum_{\alpha = VB,TB} \langle P_{lm}^{B,(\alpha)*} P_{lm}^{B,(\alpha)} \rangle &= 4\pi \int \frac{\mathrm{d}k}{k} 2 \left(\frac{k^3}{2\pi^2} P^{(VB)}(k) \right) \left| \int_0^{\eta_0} \mathrm{d}\eta g(\eta) (-\sqrt{6} \mathcal{P}^{(1)}(k,\eta)) \beta_l^{(1)}(k(\eta_0-\eta)) \right|^2 \\ &+ 4\pi \int \frac{\mathrm{d}k}{k} 2 \left(\frac{k^3}{2\pi^2} P^{(TB)}(k) \right) \left| \int_0^{\eta_0} \mathrm{d}\eta g(\eta) (-\sqrt{6} \mathcal{P}^{(2)}(k,\eta)) \beta_l^{(2)}(k(\eta_0-\eta)) \right|^2, \end{aligned} \tag{51}$$

where the tensor-to-scalar ratio is defined as $r = 2P^{(TE)}(k)/P^{(L)}(k) = 2P^{(TB)}(k)/P^{(L)}(k)$. Similarly, $C_l^{\Phi^E \Phi^E}$ and $C_l^{\Phi^B \Phi^B}$ are given by

$$\begin{aligned} C_l^{\Phi^E \Phi^E} = \sum_{\alpha = L,VE,TE} \langle \Phi_{lm}^{E,(\alpha)*} \Phi_{lm}^{E,(\alpha)} \rangle &= 4\pi A^2 \Bigg(\int \frac{\mathrm{d}k}{k} \left(\frac{k^3}{2\pi^2} P^{(L)}(k) \right) \left| \int_{\eta_{\rm LSS}}^{\eta_0} \mathrm{d}\eta (1+z)^4 (\bar{a}^E_{2,0}(k,\eta)) \epsilon_l^{(0)}(k(\eta_0-\eta)) \right|^2 \\ &+ \int \frac{\mathrm{d}k}{k} 2 \left(\frac{k^3}{2\pi^2} P^{(VE)}(k) \right) \left| \int_{\eta_{\rm LSS}}^{\eta_0} \mathrm{d}\eta (1+z)^4 (\bar{a}^E_{2,1}(k,\eta)) \epsilon_l^{(1)}(k(\eta_0-\eta)) \right|^2 \\ &+ \int \frac{\mathrm{d}k}{k} 2 \left(\frac{k^3}{2\pi^2} P^{(TE)}(k) \right) \left| \int_{\eta_{\rm LSS}}^{\eta_0} \mathrm{d}\eta (1+z)^4 (\bar{a}^E_{2,2}(k,\eta)) \epsilon_l^{(2)}(k(\eta_0-\eta)) \right|^2 \Bigg), \end{aligned} \tag{52}$$

$$\begin{aligned} C_l^{\Phi^B \Phi^B} = \sum_{\alpha = VB,TB} \langle \Phi_{lm}^{B,(\alpha)*} \Phi_{lm}^{B,(\alpha)} \rangle &= 4\pi A^2 \Bigg(\int \frac{\mathrm{d}k}{k} 2 \left(\frac{k^3}{2\pi^2} P^{(VB)}(k) \right) \left| \int_{\eta_{\rm LSS}}^{\eta_0} \mathrm{d}\eta (1+z)^4 (\bar{a}^E_{2,1}(k,\eta)) \beta_l^{(1)}(k(\eta_0-\eta)) \right|^2 \\ &+ \int \frac{\mathrm{d}k}{k} 2 \left(\frac{k^3}{2\pi^2} P^{(TB)}(k) \right) \left| \int_{\eta_{\rm LSS}}^{\eta_0} \mathrm{d}\eta (1+z)^4 (\bar{a}^E_{2,2}(k,\eta)) \beta_l^{(2)}(k(\eta_0-\eta)) \right|^2 \Bigg). \end{aligned} \tag{53}$$

The cross correlations $C_l^{P^E \Phi^E}$ and $C_l^{P^B \Phi^B}$ are also given by

$$C_l^{P^E\Phi^E} = \sum_{\alpha=L,VE,TE} \langle P_{lm}^{E,(\alpha)*}\Phi_{lm}^{E,(\alpha)}\rangle = 4\pi A\left(\int \frac{\mathrm{d}k}{k}\left(\frac{k^3}{2\pi^2}P^{(L)}(k)\right)\left(\int_{\eta_{\mathrm{LSS}}}^{\eta_0}\mathrm{d}\eta(1+z)^4(\bar{a}_{2,0}^E(k,\eta))\epsilon_l^{(0)}(k(\eta_0-\eta))\right)\right.$$
$$\times\left(\int_0^{\eta_0}\mathrm{d}\eta g(\eta)(-\sqrt{6}\mathcal{P}^{(0)}(k,\eta))\epsilon_l^{(0)}(k(\eta_0-\eta))\right)$$
$$+\int\frac{\mathrm{d}k}{k}2\left(\frac{k^3}{2\pi^2}P^{(VE)}(k)\right)\left(\int_{\eta_{\mathrm{LSS}}}^{\eta_0}\mathrm{d}\eta(1+z)^4(\bar{a}_{2,1}^E(k,\eta))\epsilon_l^{(1)}(k(\eta_0-\eta))\right)$$
$$\times\left(\int_0^{\eta_0}\mathrm{d}\eta g(\eta)(-\sqrt{6}\mathcal{P}^{(1)}(k,\eta))\epsilon_l^{(1)}(k(\eta_0-\eta))\right)$$
$$+\int\frac{\mathrm{d}k}{k}2\left(\frac{k^3}{2\pi^2}P^{(TE)}(k)\right)\left(\int_{\eta_{\mathrm{LSS}}}^{\eta_0}\mathrm{d}\eta(1+z)^4(\bar{a}_{2,2}^E(k,\eta))\epsilon_l^{(2)}(k(\eta_0-\eta))\right)$$
$$\left.\times\left(\int_0^{\eta_0}\mathrm{d}\eta g(\eta)(-\sqrt{6}\mathcal{P}^{(2)}(k,\eta))\epsilon_l^{(2)}(k(\eta_0-\eta))\right)\right), \tag{54}$$

$$C_l^{P^B\Phi^B} = \sum_{\alpha=VB,TB} \langle P_{lm}^{B,(\alpha)*}\Phi_{lm}^{B,(\alpha)}\rangle = 4\pi A\left(\int \frac{\mathrm{d}k}{k}2\left(\frac{k^3}{2\pi^2}P^{(VB)}(k)\right)\left(\int_{\eta_{\mathrm{LSS}}}^{\eta_0}\mathrm{d}\eta(1+z)^4(\bar{a}_{2,1}^E(k,\eta))\beta_l^{(1)}(k(\eta_0-\eta))\right)\right.$$
$$\times\left(\int_0^{\eta_0}\mathrm{d}\eta g(\eta)(-\sqrt{6}\mathcal{P}^{(1)}(k,\eta))\beta_l^{(1)}(k(\eta_0-\eta))\right)$$
$$+\int\frac{\mathrm{d}k}{k}2\left(\frac{k^3}{2\pi^2}P^{(TB)}(k)\right)\left(\int_{\eta_{\mathrm{LSS}}}^{\eta_0}\mathrm{d}\eta(1+z)^4(\bar{a}_{2,2}^E(k,\eta))\beta_l^{(2)}(k(\eta_0-\eta))\right)$$
$$\left.\times\left(\int_0^{\eta_0}\mathrm{d}\eta g(\eta)(-\sqrt{6}\mathcal{P}^{(2)}(k,\eta))\beta_l^{(2)}(k(\eta_0-\eta))\right)\right). \tag{55}$$

V. CALCULATION OF C_l^{VV} AND NUMERICAL RESULTS

In this section, we explain how to calculate the power spectrum C_l^{VV} for the induced circular polarization with the results derived in the previous section, and we present numerical results for a scale-invariant spectrum of primordial tensor perturbations. We follow the discussion in Ref. [25], but take into account the B mode, which is not considered in Ref. [25]. This is because, unlike scalar perturbations, vector and tensor perturbations induce B modes as we saw in the previous section.

The angular power spectrum is defined by $C_l^{VV} = \langle V_{lm}^* V_{lm}\rangle$ in terms of expansion coefficients,

$$V_{lm} = \int \mathrm{d}\hat{\boldsymbol{n}} V(\hat{\boldsymbol{n}})Y_{lm}^*(\hat{\boldsymbol{n}}). \tag{56}$$

Substituting Eqs. (6), (34), and (35) into Eq. (56), we obtain

$$V_{lm} = \sum_{l_1m_1}\sum_{l_2m_2}\left(P_{l_1m_1}^E\Phi_{l_2m_2}^E\int\mathrm{d}\hat{\boldsymbol{n}}\epsilon^{ab}Y_{(l_1m_1)ac}^E(\hat{\boldsymbol{n}})Y_{(l_2m_2)b}^{E\ \ c}(\hat{\boldsymbol{n}})Y_{lm}^*(\hat{\boldsymbol{n}}) + P_{l_1m_1}^E\Phi_{l_2m_2}^B\int\mathrm{d}\hat{\boldsymbol{n}}\epsilon^{ab}Y_{(l_1m_1)ac}^E(\hat{\boldsymbol{n}})Y_{(l_2m_2)b}^{B\ \ c}(\hat{\boldsymbol{n}})Y_{lm}^*(\hat{\boldsymbol{n}})\right.$$
$$\left.+P_{l_1m_1}^B\Phi_{l_2m_2}^E\int\mathrm{d}\hat{\boldsymbol{n}}\epsilon^{ab}Y_{(l_1m_1)ac}^B(\hat{\boldsymbol{n}})Y_{(l_2m_2)b}^{E\ \ c}(\hat{\boldsymbol{n}})Y_{lm}^*(\hat{\boldsymbol{n}}) + P_{l_1m_1}^B\Phi_{l_2m_2}^B\int\mathrm{d}\hat{\boldsymbol{n}}\epsilon^{ab}Y_{(l_1m_1)ac}^B(\hat{\boldsymbol{n}})Y_{(l_2m_2)b}^{B\ \ c}(\hat{\boldsymbol{n}})Y_{lm}^*(\hat{\boldsymbol{n}})\right)$$
$$=\sum_{l_1m_1}\sum_{l_2m_2}\left(P_{l_1m_1}^E\Phi_{l_2m_2}^E\int\mathrm{d}\hat{\boldsymbol{n}}Y_{(l_1m_1)bc}^B(\hat{\boldsymbol{n}})Y_{(l_2m_2)}^{E\ \ bc}(\hat{\boldsymbol{n}})Y_{lm}^*(\hat{\boldsymbol{n}}) + P_{l_1m_1}^E\Phi_{l_2m_2}^B\int\mathrm{d}\hat{\boldsymbol{n}}Y_{(l_1m_1)bc}^B(\hat{\boldsymbol{n}})Y_{(l_2m_2)}^{B\ \ bc}(\hat{\boldsymbol{n}})Y_{lm}^*(\hat{\boldsymbol{n}})\right.$$
$$\left.+P_{l_1m_1}^B\Phi_{l_2m_2}^E\int\mathrm{d}\hat{\boldsymbol{n}}(-1)Y_{(l_1m_1)bc}^B(\hat{\boldsymbol{n}})Y_{(l_2m_2)}^{B\ \ bc}(\hat{\boldsymbol{n}})Y_{lm}^*(\hat{\boldsymbol{n}}) + P_{l_1m_1}^B\Phi_{l_2m_2}^B\int\mathrm{d}\hat{\boldsymbol{n}}Y_{(l_1m_1)bc}^B(\hat{\boldsymbol{n}})Y_{(l_2m_2)}^{E\ \ bc}(\hat{\boldsymbol{n}})Y_{lm}^*(\hat{\boldsymbol{n}})\right), \tag{57}$$

where we have used [45] $\epsilon^{ab}Y_{(lm)ac}^E(\hat{\boldsymbol{n}}) = Y_{(lm)\ \ c}^{B\ \ b}(\hat{\boldsymbol{n}})$ and $\epsilon^{ab}Y_{(lm)ac}^B(\hat{\boldsymbol{n}}) = -Y_{(lm)\ \ c}^{E\ \ b}(\hat{\boldsymbol{n}})$. According to Refs. [45,46], we can express the integrals as

$$\int \mathrm{d}\hat{\boldsymbol{n}} Y^{B}_{(l_1 m_1)}{}^{ab}(\hat{\boldsymbol{n}}) Y^{B}_{(l_2 m_2)ab}(\hat{\boldsymbol{n}}) Y^{*}_{lm}(\hat{\boldsymbol{n}}) = \int \mathrm{d}\hat{\boldsymbol{n}} Y^{B*}_{(l_1 -m_1)}{}^{ab}(\hat{\boldsymbol{n}}) Y^{B}_{(l_2 m_2)ab}(\hat{\boldsymbol{n}}) Y_{l-m}(\hat{\boldsymbol{n}}) = \xi^{l-m}_{l_1 -m_1 l_2 m_2} H^{l}_{l_1 l_2}, \tag{58}$$

$$\int \mathrm{d}\hat{\boldsymbol{n}} Y^{E}_{(l_1 m_1)}{}^{ab}(\hat{\boldsymbol{n}}) Y^{B}_{(l_2 m_2)ab}(\hat{\boldsymbol{n}}) Y^{*}_{lm}(\hat{\boldsymbol{n}}) = \int \mathrm{d}\hat{\boldsymbol{n}} Y^{E*}_{(l_1 -m_1)}{}^{ab}(\hat{\boldsymbol{n}}) Y^{B}_{(l_2 m_2)ab}(\hat{\boldsymbol{n}}) Y_{l-m}(\hat{\boldsymbol{n}}) = i\xi^{l-m}_{l_1 -m_1 l_2 m_2} H^{l}_{l_1 l_2}, \tag{59}$$

where the result is zero unless $l_1 + l_2 + l = (\mathrm{even})$ in Eq. (58) or $l_1 + l_2 + l = (\mathrm{odd})$ in Eq. (58), and $\xi^{lm}_{l_1 m_1 l_2 m_2}$ and $H^{l}_{l_1 l_2}$ are defined in terms of Wigner 3-j symbols as

$$\xi^{lm}_{l_1 m_1 l_2 m_2} \equiv (-1)^m \sqrt{\frac{(2l_1+1)(2l+1)(2l_2+1)}{4\pi}} \begin{pmatrix} l_1 & l & l_2 \\ -m_1 & m & m_2 \end{pmatrix}, \qquad H^{l}_{l_1 l_2} \equiv \begin{pmatrix} l_1 & l & l_2 \\ 2 & 0 & -2 \end{pmatrix}. \tag{60}$$

Here, we define $G^{lm}_{l_1 m_1 l_2 m_2} = -\xi^{lm}_{l_1 -m_1, l_2 m_2} H^{l}_{l_1 l_2}$ (in agreement with the conventions of Ref. [25]). Then, using $\int \mathrm{d}\hat{\boldsymbol{n}} Y^{B}_{(l_1 m_1)}{}^{ab} Y^{E}_{(l_2 m_2)ab}(\hat{\boldsymbol{n}}) Y^{*}_{lm}(\hat{\boldsymbol{n}}) = -\int \mathrm{d}\hat{\boldsymbol{n}} Y^{E}_{(l_1 m_1)}{}^{ab} Y^{B}_{(l_2 m_2)ab}(\hat{\boldsymbol{n}}) Y^{*}_{lm}(\hat{\boldsymbol{n}})$, we rewrite Eq. (57) as

$$\begin{aligned} V_{lm} = & \sum_{l_1 m_1 l_2 m_2 (\mathrm{odd})} (P^{E}_{l_1 m_1} \Phi^{E}_{l_2 m_2} (iG^{l-m}_{l_1 m_1 l_2 m_2}) + P^{B}_{l_1 m_1} \Phi^{B}_{l_2 m_2} (iG^{l-m}_{l_1 m_1 l_2 m_2})) \\ & + \sum_{l_1 m_1 l_2 m_2 (\mathrm{even})} (P^{E}_{l_1 m_1} \Phi^{B}_{l_2 m_2} (-G^{l-m}_{l_1 m_1 l_2 m_2}) - P^{B}_{l_1 m_1} \Phi^{E}_{l_2 m_2} (-G^{l-m}_{l_1 m_1 l_2 m_2})), \end{aligned} \tag{61}$$

where the subscript (odd) and (even) means that the summation is over $l_1 + l_2 + l = (\mathrm{odd})$ and $l_1 + l_2 + l = (\mathrm{even})$, respectively. Then we derive

$$\begin{aligned} C^{VV}_{l} = & \sum_{l_1 m_1 l_2 m_2 (\mathrm{odd})} [(C^{P^E P^E}_{l_1} C^{\Phi^E \Phi^E}_{l_2} - C^{P^E \Phi^E}_{l_1} C^{P^E \Phi^E}_{l_2}) + (C^{P^B P^B}_{l_1} C^{\Phi^B \Phi^B}_{l_2} - C^{P^B \Phi^B}_{l_1} C^{P^B \Phi^B}_{l_2})] |G^{l-m}_{l_1 m_1 l_2 m_2}|^2 \\ & + \sum_{l_1 m_1 l_2 m_2 (\mathrm{even})} (C^{P^E P^E}_{l_1} C^{\Phi^B \Phi^B}_{l_2} + C^{P^B P^B}_{l_1} C^{\Phi^E \Phi^E}_{l_2} - 2C^{P^E \Phi^E}_{l_1} C^{P^B \Phi^B}_{l_2}) |G^{l-m}_{l_1 m_1 l_2 m_2}|^2 \end{aligned} \tag{62}$$

$$\begin{aligned} = & \sum_{l_1 l_2 (\mathrm{odd})} \frac{(2l_1+1)(2l_2+1)}{4\pi} ((C^{P^E P^E}_{l_1} C^{\Phi^E \Phi^E}_{l_2} - C^{P^E \Phi^E}_{l_1} C^{P^E \Phi^E}_{l_2}) \\ & + (C^{P^B P^B}_{l_1} C^{\Phi^B \Phi^B}_{l_2} - C^{P^B \Phi^B}_{l_1} C^{P^B \Phi^B}_{l_2})) |H^{l}_{l_1 l_2}|^2 \\ & + \sum_{l_1 l_2 (\mathrm{even})} \frac{(2l_1+1)(2l_2+1)}{4\pi} (C^{P^E P^E}_{l_1} C^{\Phi^B \Phi^B}_{l_2} + C^{P^B P^B}_{l_1} C^{\Phi^E \Phi^E}_{l_2} - 2C^{P^E \Phi^E}_{l_1} C^{P^B \Phi^B}_{l_2}) |H^{l}_{l_1 l_2}|^2 \end{aligned} \tag{63}$$

$$\begin{aligned} \simeq & \int \frac{\mathrm{d}^2 l_1}{(2\pi)^2} \sin^2 2\varphi_{\boldsymbol{l}_1, \boldsymbol{l}-\boldsymbol{l}_1} ((C^{P^E P^E}_{l_1} C^{\Phi^E \Phi^E}_{|\boldsymbol{l}-\boldsymbol{l}_1|} - C^{P^E \Phi^E}_{l_1} C^{P^E \Phi^E}_{|\boldsymbol{l}-\boldsymbol{l}_1|}) + (C^{P^B P^B}_{l_1} C^{\Phi^B \Phi^B}_{|\boldsymbol{l}-\boldsymbol{l}_1|} - C^{P^B \Phi^B}_{l_1} C^{P^B \Phi^B}_{|\boldsymbol{l}-\boldsymbol{l}_1|})) \\ & + \int \frac{\mathrm{d}^2 l_1}{(2\pi)^2} \cos^2 2\varphi_{\boldsymbol{l}_1, \boldsymbol{l}-\boldsymbol{l}_1} (C^{P^E P^E}_{l_1} C^{\Phi^B \Phi^B}_{|\boldsymbol{l}-\boldsymbol{l}_1|} + C^{P^B P^B}_{l_1} C^{\Phi^E \Phi^E}_{|\boldsymbol{l}-\boldsymbol{l}_1|} - 2C^{P^E \Phi^E}_{l_1} C^{P^B \Phi^B}_{|\boldsymbol{l}-\boldsymbol{l}_1|}), \end{aligned} \tag{64}$$

where we have used $\sum_{m_1 m_2} (\xi^{lm}_{l_1 m_1 l_2 m_2})^2 = (2l+1)(2l'+1)/(4\pi)$ [45,46] between the first equality and second equality and we have used [45]

$$\sum_{l_1 l_2 (\mathrm{odd})} \frac{(2l+1)(2l'+1)}{4\pi} |H^{l}_{l_1 l_2}|^2 \simeq \int \frac{\mathrm{d}^2 l_1}{(2\pi)^2} \int \frac{\mathrm{d}^2 l_2}{(2\pi)^2} (2\pi)^2 \sin^2 2\varphi_{\boldsymbol{l}_1, \boldsymbol{l}_2} \delta(\boldsymbol{l} - (\boldsymbol{l}_1 + \boldsymbol{l}_2)), \tag{65}$$

$$\sum_{l_1 l_2 (\mathrm{even})} \frac{(2l+1)(2l'+1)}{4\pi} |H^{l}_{l_1 l_2}|^2 \simeq \int \frac{\mathrm{d}^2 l_1}{(2\pi)^2} \int \frac{\mathrm{d}^2 l_2}{(2\pi)^2} (2\pi)^2 \cos^2 2\varphi_{\boldsymbol{l}_1, \boldsymbol{l}_2} \delta(\boldsymbol{l} - (\boldsymbol{l}_1 + \boldsymbol{l}_2)), \tag{66}$$

valid when $l, l_1, l_2 \gg 1$, between the second and third equality.

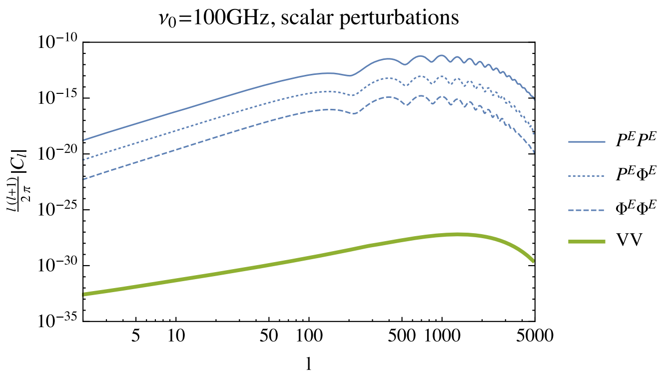

FIG. 1. The power spectra C_l for scalar perturbations. The blue solid curve shows $C_l^{P^E P^E}$; the blue dotted curve shows $|C_l^{P^E \Phi^E}|$; the blue dashed curve shows $C_l^{\Phi^E \Phi^E}$; and the green thick solid curve shows C_l^{VV}. We take $\nu_0 = 100$ GHz.

The variance of V is given by $\langle V^2 \rangle = \sum_l (2l+1) C_l^{VV}/(4\pi)$, which can be approximated,

$$\langle V^2 \rangle \simeq \int \frac{\mathrm{d}^2 l}{(2\pi)^2} C_l^{VV} \simeq \frac{1}{2}(\langle P^E P^E \rangle \langle \Phi^E \Phi^E \rangle - \langle P^E \Phi^E \rangle^2 + \langle P^B P^B \rangle \langle \Phi^B \Phi^B \rangle - \langle P^B \Phi^B \rangle^2 + \langle P^E P^E \rangle \langle \Phi^B \Phi^B \rangle + \langle P^B P^B \rangle \langle \Phi^E \Phi^E \rangle - 2 \langle P^E \Phi^E \rangle \langle P^B \Phi^B \rangle). \tag{67}$$

Finally, we provide results of numerical calculations for a scale-invariant spectrum of primordial gravitational waves, using CLASS [47] to obtain the CMB polarization transfer functions. Figures 1, and 2 show C_l^{PP}, $C_l^{P\Phi}$, $C_l^{\Phi\Phi}$, and C_l^{VV} with scalar and tensor perturbations. We take $\nu_0 = 100$ GHz for both sets of perturbations. From Eq. (67), we find the root-variance of V to be

$$\sqrt{\langle V^2 \rangle} \sim \begin{cases} 3 \times 10^{-14} & \text{(for scalar perturbations)}, \\ 7 \times 10^{-18} (\frac{r}{0.06}) & \text{(for tensor perturbations)}, \end{cases} \tag{68}$$

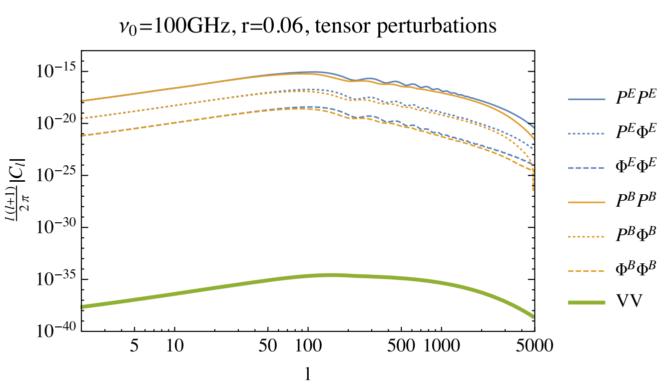

FIG. 2. The power spectra C_l for tensor perturbations. The blue and green curves are as in Fig. 1, but we now also have orange curves to indicate the analogous quantities for B modes.

or in temperature units,

$$\sqrt{\langle V^2 \rangle} \sim \begin{cases} 8 \times 10^{-14}\ \mathrm{K} & \text{(for scalar perturbations)}, \\ 2 \times 10^{-17} (\frac{r}{0.06})\ \mathrm{K} & \text{(for tensor perturbations)}. \end{cases} \tag{69}$$

From Eqs. (68) and (69), we can see that the circular polarization induced by tensor perturbations through the photon-photon scattering is much larger than that induced through the photon-graviton scattering [36].

VI. CONCLUSIONS

We have used the TAM formalism to discuss the CMB circular polarization induced at second order in the primordial-perturbation amplitude, by general primordial perturbations, including vector and tensor perturbations in addition to scalar perturbations. To make the discussion concrete, we have assumed the standard cosmology and considered only the dominant contribution—from photon-photon scattering—to Faraday conversion. We performed numerical calculations of the power spectra for circular polarization and find root-variances of $\sqrt{\langle V^2 \rangle} \sim 3 \times 10^{-14}$ for scalar perturbations, and $\sqrt{\langle V^2 \rangle} \sim 7 \times 10^{-18} (r/0.06)$ for tensor perturbations. The derived formulas can be applied to the other source terms discussed in Ref. [24] such as spin polarization of neutral hydrogen atoms and the nonlinear interactions induced by bounded or free electrons, although these are expected to be subdominant to the photon-photon process considered here.

Before closing, we note that it follows from Eq. (61) that the monopole $V_{l=0,m=0} = 0$ if there are no primordial vector or tensor modes (and thus no B modes). In other words, there will be circular-polarization fluctuations, but the mean value of the circular polarization, averaged over the entire sky, will be zero. We also note that here we have assumed that parity is conserved and thus that there are no correlations between the TE and TB TAM modes. An accompanying [48] paper shows that the TE/TB cross-correlations that arise if parity is broken may allow for a parity-breaking uniform (averaged over all directions) circular polarization $V_{l=0,m=0}$. The paper also shows that a uniform circular polarization may arise even in the absence of parity-breaking physics through a realization of a gravitational-wave field that spontaneously breaks parity.

ACKNOWLEDGMENTS

We thank Paulo Montero-Camacho for useful comments. K. I. is supported by World Premier International Research Center Initiative (WPI Initiative), MEXT, Japan, Advanced Leading Graduate Course for Photon Science, and JSPS Research Fellowship for Young Scientists, and thanks Johns Hopkins University for hospitality. This work was supported at Johns Hopkins in part by NASA Grant No. NNX17AK38G, NSF Grant No. 1818899, and the Simons Foundation.

APPENDIX A: WIGNER ROTATION MATRICES

Here, we review some useful properties of the Wigner rotation matrices, using the notation [49]

$$D^l_{m',m}(\alpha,\beta,\gamma) = \sum_{s=\max[0,m-m']}^{\min[l+m,l-m']} (-1)^s \frac{\sqrt{(l+m)!(l-m)!(l+m')!(l-m')!}}{(l-m'-s)!(l+m-s)!s!(s+m'-m)!} \times e^{im'\alpha}\left(\cos\frac{\beta}{2}\right)^{2l+m-m'-2s}\left(\sin\frac{\beta}{2}\right)^{2s+m'-m} e^{im\gamma}. \tag{A1}$$

The relations between the spherical harmonics in the line-of-sight frame (θ',ϕ') and the wave-vector frame (θ,ϕ) are given by [49]

$$Y^*_{lm}(\theta',\phi') = \sum_k D^l_{mk}(\pi-\phi_{\boldsymbol{k}},\theta_{\boldsymbol{k}},0)Y^*_{lk}(\theta,\phi). \tag{A2}$$

Since the coefficients are given by $a^A_{lm} = \int d\hat{\boldsymbol{n}} A(\hat{\boldsymbol{n}})Y^*_{lm}(\hat{\boldsymbol{n}})$, the relation between the coefficients of spherical harmonics in the two frames is

$$a^E_{lm}(\boldsymbol{k},\eta) = \sum_k D^l_{mk}(\pi-\phi_{\boldsymbol{k}},\theta_{\boldsymbol{k}},0)\bar{a}^E_{lk}(\boldsymbol{k},\eta). \tag{A3}$$

APPENDIX B: PHOTON-PHOTON SCATTERING

Here, we derive Eqs. (24) and (25). For photons with energies far smaller than the electron rest-mass energy, the effective Lagrangian for the electromagnetic field can be approximated as the Euler-Heisenberg Lagrangian [50][5]

$$\mathcal{L} \simeq \frac{1}{2\mu_0}\left(\frac{\boldsymbol{E}\cdot\boldsymbol{E}}{c^2} - \boldsymbol{B}\cdot\boldsymbol{B}\right) + \frac{A_e}{\mu_0}\left[\left(\frac{\boldsymbol{E}\cdot\boldsymbol{E}}{c^2} - \boldsymbol{B}\cdot\boldsymbol{B}\right)^2 + 7\left(\frac{\boldsymbol{E}\cdot\boldsymbol{B}}{c}\right)^2\right]. \tag{B1}$$

By using the constitutive relations $\boldsymbol{D} = \partial\mathcal{L}/\partial\boldsymbol{E}$ and $\boldsymbol{H} = -\partial\mathcal{L}/\partial\boldsymbol{B}$, we obtain

$$\boldsymbol{D} = \epsilon_0\boldsymbol{E} + \epsilon_0 A_e\left[4\left(\frac{\boldsymbol{E}\cdot\boldsymbol{E}}{c^2} - \boldsymbol{B}\cdot\boldsymbol{B}\right)\boldsymbol{E} + 14(\boldsymbol{E}\cdot\boldsymbol{B})\boldsymbol{B}\right], \tag{B2}$$

$$\boldsymbol{H} = \frac{\boldsymbol{B}}{\mu_0} + \frac{A_e}{\mu_0}\left[4\left(\frac{\boldsymbol{E}\cdot\boldsymbol{E}}{c^2} - \boldsymbol{B}\cdot\boldsymbol{B}\right)\boldsymbol{B} - 14\frac{(\boldsymbol{E}\cdot\boldsymbol{B})}{c^2}\boldsymbol{E}\right], \tag{B3}$$

where $\boldsymbol{D}$ is the electric-displacement vector and $\boldsymbol{H}$ is the magnetic-intensity vector. To consider the interaction between the propagating photon and background radiation, we write the electric and magnetic fields as

$$\boldsymbol{E} = \boldsymbol{E}_A e^{i(\boldsymbol{k}\cdot\boldsymbol{x}-\omega t)} + \boldsymbol{E}^*_A e^{-i(\boldsymbol{k}\cdot\boldsymbol{x}-\omega t)} + \boldsymbol{E}_B(\boldsymbol{x},t), \qquad \boldsymbol{B} = \boldsymbol{B}_A e^{i(\boldsymbol{k}\cdot\boldsymbol{x}-\omega t)} + \boldsymbol{B}^*_A e^{-i(\boldsymbol{k}\cdot\boldsymbol{x}-\omega t)} + \boldsymbol{B}_B(\boldsymbol{x},t), \tag{B4}$$

where $\boldsymbol{E}_A$ and $\boldsymbol{B}_A$ are the electromagnetic fields associated with the propagating photon and $\boldsymbol{E}_B$ and $\boldsymbol{B}_B$ are those associated with the background radiation. We assume $\boldsymbol{B}^A_i = \epsilon_{ijk}\hat{k}^k\boldsymbol{E}^j_A$, where ϵ_{ijk} is the Levi-Civita symbol. From Eqs. (B2)–(B4), we find that

[5]In this paper, we assume the standard model. If we assume new particles, such as axionlike particles, the coefficients in the Lagrangian could be changed [51].

$$D_i \simeq \mathrm{e}^{i(\boldsymbol{k}\cdot\boldsymbol{x}-\omega t)}\epsilon_0\left(\delta_{ij} + A_e\left[4\left(\frac{\langle \boldsymbol{E_B}\cdot\boldsymbol{E_B}\rangle}{c^2} - \langle \boldsymbol{B_B}\cdot\boldsymbol{B_B}\rangle\right)\delta_{ij} + 8\frac{\langle E_i^B E_j^B\rangle}{c^2} + 14\langle B_i^B B_j^B\rangle\right]\right)E_A^j + \cdots, \tag{B5}$$

$$H_i \simeq \mathrm{e}^{i(\boldsymbol{k}\cdot\boldsymbol{x}-\omega t)}\frac{1}{\mu_0}\left(\delta_{ij} - (-1)A_e\left[4\left(\frac{\langle \boldsymbol{E_B}\cdot\boldsymbol{E_B}\rangle}{c^2} - \langle \boldsymbol{B_B}\cdot\boldsymbol{B_B}\rangle\right)\delta_{ij} - 8\langle B_i^B B_j^B\rangle - 14\frac{\langle E_i^B E_j^B\rangle}{c^2}\right]\right)\epsilon^{jkl}\hat{k}_k E_l^A + \cdots, \tag{B6}$$

where we explicitly write only the terms proportional to $\mathrm{e}^{i(\boldsymbol{k}\cdot\boldsymbol{x}-\omega t)}$, and $\langle\cdots\rangle$ means the expectation value of the stochastic background radiation. Then, we derive

$$\chi_{e,ij} \simeq A_e\left[4\left(\frac{\langle \boldsymbol{E_B}\cdot\boldsymbol{E_B}\rangle}{c^2} - \langle \boldsymbol{B_B}\cdot\boldsymbol{B_B}\rangle\right)\delta_{ij} + 8\frac{\langle E_i^B E_j^B\rangle}{c^2} + 14\langle B_i^B B_j^B\rangle\right], \tag{B7}$$

$$\chi_{m,ij} \simeq -A_e\left[4\left(\frac{\langle \boldsymbol{E_B}\cdot\boldsymbol{E_B}\rangle}{c^2} - \langle \boldsymbol{B_B}\cdot\boldsymbol{B_B}\rangle\right)\delta^{kl} - 8\langle B_B^k B_B^l\rangle - 14\frac{\langle E_B^k E_B^l\rangle}{c^2}\right]\epsilon_{kmi}\hat{k}^m\epsilon_{lnj}\hat{k}^n. \tag{B8}$$

From Eqs. (B7) and (B8), we obtain

$$n_{xx}(\boldsymbol{x},t) - n_{yy}(\boldsymbol{x},t) = \frac{1}{2}(\chi_{e,xx} + \chi_{m,xx} - \chi_{e,yy} - \chi_{m,yy}) = 3A_e\left(\langle B_x^B B_x^B\rangle - \langle B_y^B B_y^B\rangle - \frac{1}{c^2}(\langle E_x^B E_x^B\rangle - \langle E_y^B E_y^B\rangle)\right) \tag{B9}$$

$$n_{xy}(\boldsymbol{x},t) = \frac{1}{2}(\chi_{e,xy} + \chi_{m,xy}) = 3A_e\left(\langle B_x^B B_y^B\rangle - \frac{1}{c^2}\langle E_x^B E_y^B\rangle\right). \tag{B10}$$

Here, we expand the background electric and magnetic field with creation and annihilation operators as

$$E_i^B(\boldsymbol{x},t) = i\int\frac{\mathrm{d}^3p}{(2\pi)^3}\sum_{\alpha=x,y}\sqrt{\frac{U_p}{2\epsilon_0}}\hat{\boldsymbol{e}}_i^\alpha(a_\alpha(\boldsymbol{p})\mathrm{e}^{i(\boldsymbol{p}\cdot\boldsymbol{x}-\omega t)} - a_\alpha^\dagger(\boldsymbol{p})\mathrm{e}^{-i(\boldsymbol{p}\cdot\boldsymbol{x}-\omega t)}), \tag{B11}$$

$$B_i^B(\boldsymbol{x},t) = i\int\frac{\mathrm{d}^3p}{(2\pi)^3}\sum_{\alpha=x,y}\sqrt{\frac{U_p}{2\epsilon_0 c^2}}(\hat{\boldsymbol{p}}\times\hat{\boldsymbol{e}}_i^\alpha)(a_\alpha(\boldsymbol{p})\mathrm{e}^{i(\boldsymbol{p}\cdot\boldsymbol{x}-\omega t)} - a_\alpha^\dagger(\boldsymbol{p})\mathrm{e}^{-i(\boldsymbol{p}\cdot\boldsymbol{x}-\omega t)}), \tag{B12}$$

where we define the basis vectors as $\hat{\boldsymbol{e}}^x \equiv \hat{\boldsymbol{\theta}}$ and $\hat{\boldsymbol{e}}^y \equiv \hat{\boldsymbol{\phi}}$. The expectation value of photon number density is described with a phase-space density matrix as

$$\langle a_\alpha^\dagger(\boldsymbol{p})a_\beta(\boldsymbol{p}')\rangle_{\boldsymbol{x},t} = (2\pi)^3\delta(\boldsymbol{p}-\boldsymbol{p}')f_{\alpha\beta}(\boldsymbol{p},\boldsymbol{x},t), \tag{B13}$$

where the subscript $\boldsymbol{x}$ and t indicate the spacetime point in which we consider the expectation value, and from Ref. [52],

$$f_{\alpha\beta}(\boldsymbol{p},\boldsymbol{x},t) = \begin{pmatrix} f_I(\boldsymbol{p},\boldsymbol{x},t) + f_Q(\boldsymbol{p},\boldsymbol{x},t) & f_U(\boldsymbol{p},\boldsymbol{x},t) - if_V(\boldsymbol{p},\boldsymbol{x},t) \\ f_U(\boldsymbol{p},\boldsymbol{x},t) + if_V(\boldsymbol{p},\boldsymbol{x},t) & f_I(\boldsymbol{p},\boldsymbol{x},t) - f_Q(\boldsymbol{p},\boldsymbol{x},t) \end{pmatrix}. \tag{B14}$$

Substituting Eqs. (B11) and (B12) into Eqs. (B9) and (B10), we obtain

$$\begin{aligned} n_Q(\boldsymbol{x},t) &= \frac{1}{2}(n_{xx}(\boldsymbol{x},t) - n_{yy}(\boldsymbol{x},t)) \\ &= -\frac{3A_e}{2\epsilon_0 c^2}\sqrt{\frac{\pi}{5}}\int\frac{U_p}{2}p^2\mathrm{d}p\int\mathrm{d}^2\hat{\boldsymbol{p}}[4f_Q(\boldsymbol{p},\boldsymbol{x},t)(1+\cos^2\theta_{\boldsymbol{p}})\cos 2\phi - 8f_U(\boldsymbol{p},\boldsymbol{x},t)\cos\theta_{\boldsymbol{p}}\sin 2\phi_{\boldsymbol{p}}] \\ &= -\frac{24A_e}{\epsilon_0 c^2}\sqrt{\frac{\pi}{5}}\int\frac{U_p}{2}p^2\mathrm{d}p\int\mathrm{d}^2\hat{\boldsymbol{p}}[f_Q(\boldsymbol{p},\boldsymbol{x},t)\mathrm{Re}\{{}_2Y_{22}(\hat{\boldsymbol{p}}) + {}_2Y_{2,-2}(\hat{\boldsymbol{p}})\} + f_U(\boldsymbol{p},\boldsymbol{x},t)\mathrm{Im}\{{}_2Y_{22}(\hat{\boldsymbol{p}}) + {}_2Y_{2,-2}(\hat{\boldsymbol{p}})\}] \\ &= 48\sqrt{\frac{\pi}{5}}A_e\mu_0 a_{\mathrm{rad}}T_{\mathrm{CMB}}^4\mathrm{Re}a_{2,-2}^E(\boldsymbol{x},t), \end{aligned} \tag{B15}$$

$$\begin{aligned} n_U(\boldsymbol{x},t) &= \frac{1}{2}(n_{xy}(\boldsymbol{x},t) + n_{yx}(\boldsymbol{x},t)) \\ &= -\frac{3A_e}{2\epsilon_0 c^2}\sqrt{\frac{\pi}{5}}\int \frac{U_p}{2}p^2 \mathrm{d}p \int \mathrm{d}^2\hat{\boldsymbol{p}}[4f_Q(\boldsymbol{p},\boldsymbol{x},t)(1+\cos^2\theta_{\boldsymbol{p}})\sin 2\phi_{\boldsymbol{p}} + 8f_U(\boldsymbol{p},\boldsymbol{x},t)\cos\theta_{\boldsymbol{p}}\cos 2\phi_{\boldsymbol{p}}] \\ &= -\frac{24A_e}{\epsilon_0 c^2}\sqrt{\frac{\pi}{5}}\int \frac{U_p}{2}p^2 \mathrm{d}p \int \mathrm{d}^2\hat{\boldsymbol{p}}[f_Q(\boldsymbol{p},\boldsymbol{x},t)\mathrm{Im}\{{}_2Y_{22}(\hat{\boldsymbol{p}}) - {}_2Y_{2,-2}(\hat{\boldsymbol{p}})\} - f_U(\boldsymbol{p},\boldsymbol{x},t)\mathrm{Re}\{{}_2Y_{22}(\hat{\boldsymbol{p}}) -{}_2 Y_{2,-2}(\hat{\boldsymbol{p}})\}] \\ &= 48\sqrt{\frac{\pi}{5}}A_e\mu_0 a_{\mathrm{rad}} T^4_{\mathrm{CMB}}\mathrm{Im}a^E_{2,-2}(\boldsymbol{x},t), \end{aligned} \tag{B16}$$

where $\theta_{\boldsymbol{p}}$ and $\phi_{\boldsymbol{p}}$ are the polar and azimuthal angles of $\hat{\boldsymbol{p}}$ in the line-of-sight frame, and we have used [53],

$$f_Q(\boldsymbol{p},\boldsymbol{x},t) = Q(\hat{\boldsymbol{p}},\boldsymbol{x},t)(-p\partial f^{(0)}/\partial p), \qquad f_U(\boldsymbol{p},\boldsymbol{x},t) = U(\hat{\boldsymbol{p}},\boldsymbol{x},t)(-p\partial f^{(0)}/\partial p), \tag{B17}$$

$$Q(\hat{\boldsymbol{p}},\boldsymbol{x},t) = \frac{1}{2}\sum_{l,m}(a_{2,lm}(\boldsymbol{x},t)_2Y_{lm}(\hat{\boldsymbol{p}}) + a_{-2,lm}(\boldsymbol{x},t)_{-2}Y_{lm}(\hat{\boldsymbol{p}})), \tag{B18}$$

$$U(\hat{\boldsymbol{p}},\boldsymbol{x},t) = \frac{1}{2i}\sum_{l,m}(a_{2,lm}(\boldsymbol{x},t)_2Y_{lm}(\hat{\boldsymbol{p}}) - a_{-2,lm}(\boldsymbol{x},t)_{-2}Y_{lm}(\hat{\boldsymbol{p}})), \tag{B19}$$

$${}_sY_{lm}(\hat{\boldsymbol{p}}) = {}_{-s}Y^*_{l,-m}(\hat{\boldsymbol{p}}), \qquad a^E_{lm}(\boldsymbol{x},t) = -\frac{1}{2}(a_{2,lm}(\boldsymbol{x},t) + a_{-2,lm}(\boldsymbol{x},t)). \tag{B20}$$

If we take the conformal spacetime, Eqs. (B15) and (B16) correspond to Eqs. (24) and (25).

---

[1] N. Aghanim *et al.* (Planck Collaboration), Planck 2018 results. VI. Cosmological parameters, arXiv:1807.06209.
[2] W. Hu and M. J. White, A CMB polarization primer, New Astron. **2**, 323 (1997).
[3] M. Kamionkowski and E. D. Kovetz, The Quest for B modes from inflationary gravitational waves, Annu. Rev. Astron. Astrophys. **54**, 227 (2016).
[4] K. N. Abazajian *et al.* (CMB-S4 Collaboration), CMB-S4 Science Book, 1st ed., arXiv:1610.02743.
[5] J. Chluba, J. Hamann, and S. P. Patil, Features and new physical scales in primordial observables: Theory and observation, Int. J. Mod. Phys. D **24**, 1530023 (2015).
[6] S. Deguchi and W. Watson, Circular polarization of astrophysical masers due to overlap of Zeeman components, Astrophys. J. **300**, L15 (1986).
[7] W. D. Watson and H. W. Wyld, The relationship between the circular polarization and the magnetic field for astrophysical masers with weak zeeman splitting, Astrophys. J. **558**, L55 (2001).
[8] M. Matsumiya and K. Ioka, Circular polarization from gamma-ray burst afterglows, Astrophys. J. **595**, L25 (2003).
[9] K. Wiersema *et al.*, Circular polarization in the optical afterglow of GRB 121024A, Nature (London) **509**, 201 (2014).
[10] S. Batebi, R. Mohammadi, R. Ruffini, S. Tizchang, and S. S. Xue, Generation of circular polarization of gamma ray bursts, Phys. Rev. D **94**, 065033 (2016).
[11] S. Shakeri and A. Allahyari, Circularly polarized EM radiation from GW binary sources, J. Cosmol. Astropart. Phys. 11 (2018) 042.
[12] A. Brunthaler, G. C. Bower, H. Falcke, and R. R. Mellon, Detection of circular polarization in M81*, Astrophys. J. **560**, L123 (2001).
[13] D. C. Homan, M. L. Lister, H. D. Aller, M. F. Aller, and J. F. C. Wardle, Full polarization spectra of 3C 279, Astrophys. J. **696**, 328 (2009).
[14] D. C. Homan, J. M. Attridge, and J. F. C. Wardle, Parsec-scale circular polarization observations of 40 blazars, Astrophys. J. **556**, 113 (2001).
[15] T. Beckert and H. Falcke, Circular polarization of radio emission from relativistic jets, Astron. Astrophys. **388**, 1106 (2002).
[16] A. Karastergiou, S. Johnston, D. Mitra, A. G. J. van Leeuwen, and R. T. Edwards, V: New insight into the circular polarization of radio pulsars, Mon. Not. R. Astron. Soc. **344**, L69 (2003).
[17] D. Melrose, in *Radio Pulsars* (Astronomical Society of the Pacific, San Francisco, 2003), Vol. 302, p. 179.

[18] D. Mitra, J. Gil, and G. I. Melikidze, Unraveling the nature of coherent pulsar radio emission, Astrophys. J. **696**, L141 (2009).

[19] S. Shakeri, M. Haghighat, and S. S. Xue, Nonlinear QED effects in X-ray emission of pulsars, J. Cosmol. Astropart. Phys. 10 (2017) 014.

[20] E. Bavarsad, M. Haghighat, Z. Rezaei, R. Mohammadi, I. Motie, and M. Zarei, Generation of circular polarization of the CMB, Phys. Rev. D **81**, 084035 (2010).

[21] S. Tizchang, S. Batebi, M. Haghighat, and R. Mohammadi, Cosmic microwave background polarization in noncommutative space-time, Eur. Phys. J. C **76**, 478 (2016).

[22] S. De and H. Tashiro, Circular polarization of the CMB: A probe of the first stars, Phys. Rev. D **92**, 123506 (2015).

[23] S. King and P. Lubin, Circular polarization of the CMB: Foregrounds and detection prospects, Phys. Rev. D **94**, 023501 (2016).

[24] P. Montero-Camacho and C. M. Hirata, Exploring circular polarization in the CMB due to conventional sources of cosmic birefringence, J. Cosmol. Astropart. Phys. 08 (2018) 040.

[25] M. Kamionkowski, Circular polarization in a spherical basis, Phys. Rev. D **97**, 123529 (2018).

[26] R. B. Partridge, J. Nowakowski, and H. M. Martin, Linear polarized fluctuations in the cosmic microwave background, Nature (London) **331**, 146 (1988).

[27] J. M. Nagy *et al.* (SPIDER Collaboration), A New limit on CMB circular polarization from SPIDER, Astrophys. J. **844**, 151 (2017).

[28] R. Mainini, D. Minelli, M. Gervasi, G. Boella, G. Sironi, A. Baú, S. Banfi, A. Passerini, A. De Lucia, and F. Cavaliere, An improved upper limit to the CMB circular polarization at large angular scales, J. Cosmol. Astropart. Phys. 08 (2013) 033.

[29] T. Essinger-Hileman *et al.*, CLASS: The cosmology large angular scale surveyor, Proc. SPIE Int. Soc. Opt. Eng. **9153**, 91531I (2014).

[30] J. Lazear *et al.*, The Primordial Inflation Polarization Explorer (PIPER), Proc. SPIE Int. Soc. Opt. Eng. **9153**, 91531L (2014).

[31] I. Motie and S. S. Xue, Euler-Heisenberg lagrangian and photon circular polarization, Europhys. Lett. **100**, 17006 (2012).

[32] R. F. Sawyer, Photon-photon interactions can be a source of CMB circular polarization, arXiv:1408.5434.

[33] D. Ejlli, Magneto-optic effects of the cosmic microwave background, Nucl. Phys. **B935**, 83 (2018).

[34] S. Shakeri, S. Z. Kalantari, and S. S. Xue, Polarization of a probe laser beam due to nonlinear QED effects, Phys. Rev. A **95**, 012108 (2017).

[35] M. Sadegh, R. Mohammadi, and I. Motie, Generation of circular polarization in CMB radiation via nonlinear photon-photon interaction, Phys. Rev. D **97**, 023023 (2018).

[36] N. Bartolo, A. Hoseinpour, G. Orlando, S. Matarrese, and M. Zarei, Photon-graviton scattering: A new way to detect anisotropic gravitational waves?, Phys. Rev. D **98**, 023518 (2018).

[37] L. Dai, M. Kamionkowski, and D. Jeong, Total angular momentum waves for scalar, vector, and tensor fields, Phys. Rev. D **86**, 125013 (2012).

[38] L. Dai, D. Jeong, and M. Kamionkowski, Wigner-Eckart theorem in cosmology: Bispectra for total-angular-momentum waves, Phys. Rev. D **87**, 043504 (2013).

[39] E. Newman and R. Penrose, An approach to gravitational radiation by a method of spin coefficients, J. Math. Phys. **3**, 566 (1962).

[40] J. N. Goldberg, A. J. MacFarlane, E. T. Newman, F. Rohrlich, and E. C. G. Sudarshan, Spin s spherical harmonics and edth, J. Math. Phys. **8**, 2155 (1967).

[41] W. Hu and M. J. White, CMB anisotropies: Total angular momentum method, Phys. Rev. D **56**, 596 (1997).

[42] M. Kamionkowski, A. Kosowsky, and A. Stebbins, Statistics of cosmic microwave background polarization, Phys. Rev. D **55**, 7368 (1997).

[43] M. Zaldarriaga and U. Seljak, An all sky analysis of polarization in the microwave background, Phys. Rev. D **55**, 1830 (1997).

[44] T. Tram and J. Lesgourgues, Optimal polarisation equations in FLRW universes, J. Cosmol. Astropart. Phys. 10 (2013) 002.

[45] V. Gluscevic, M. Kamionkowski, and A. Cooray, Derotation of the cosmic microwave background polarization: Full-sky formalism, Phys. Rev. D **80**, 023510 (2009).

[46] W. Hu, Weak lensing of the CMB: A harmonic approach, Phys. Rev. D **62**, 043007 (2000).

[47] D. Blas, J. Lesgourgues, and T. Tram, The cosmic linear anisotropy solving system (CLASS) II: Approximation schemes, J. Cosmol. Astropart. Phys. 07 (2011) 034.

[48] K. Inomata and M. Kamionkowski, Chiral photons from chiral gravitational waves, arXiv:1811.04959.

[49] E. Wigner, *Group theory: And its application to the quantum mechanics of atomic spectra* (Elsevier, Amsterdam, 2012), Vol. 5.

[50] W. Heisenberg and H. Euler, Folgerungen aus der Diracschen Theorie des Positrons, Z. Phys. **98**, 714 (1936).

[51] G. Zavattini, U. Gastaldi, R. Pengo, G. Ruoso, F. Della Valle, and E. Milotti, Measuring the magnetic birefringence of vacuum: the PVLAS experiment, Int. J. Mod. Phys. A **27**, 1260017 (2012).

[52] A. Kosowsky, Cosmic microwave background polarization, Ann. Phys. (N.Y.) **246**, 49 (1996).

[53] Y. T. Lin and B. D. Wandelt, A Beginner's guide to the theory of CMB temperature and polarization power spectra in the line-of-sight formalism, Astropart. Phys. **25**, 151 (2006).